

Simplified Models vs. Effective Field Theory Approaches in Dark Matter Searches

Andrea De Simone ¹, Thomas Jacques ¹

¹SISSA and INFN Sezione di Trieste, via Bonomea 265, I-34136 Trieste, Italy
E-mail: andrea.desimone@sissa.it, thomas.jacques@sissa.it

25 March 2016

Abstract In this review we discuss and compare the usage of simplified models and Effective Field Theory (EFT) approaches in dark matter searches. We provide a state of the art description on the subject of EFTs and simplified models, especially in the context of collider searches for dark matter, but also with implications for direct and indirect detection searches, with the aim of constituting a common language for future comparisons between different strategies. The material is presented in a form that is as self-contained as possible, so that it may serve as an introductory review for the newcomer as well as a reference guide for the practitioner.

Contents

1	Introduction	2
2	Effective Field Theories: virtues and drawbacks	4
2.1	Effective Field Theories for collider searches	5
2.2	Effective Field Theories for direct detection	9
2.3	Effective Field Theories for indirect detection	15
3	A paradigm shift: Simplified Models	16
3.1	General properties of simplified models	17
3.2	Scalar Mediator	18
3.2.1	Scalar DM, <i>s</i> -channel ($0s0$ model)	19
3.2.2	Fermion DM, <i>s</i> -channel ($0s\frac{1}{2}$ model)	20
3.2.3	Scalar DM, <i>t</i> -channel ($0t0$ model)	27
3.2.4	Fermion DM, <i>t</i> -channel ($0t\frac{1}{2}$ model)	27
3.3	Fermion Mediator	31
3.3.1	Scalar DM, <i>t</i> -channel ($\frac{1}{2}t0$ model)	31
3.3.2	Fermion DM, <i>t</i> -channel ($\frac{1}{2}t\frac{1}{2}$ model)	33
3.4	Vector Mediator	33
3.4.1	Scalar DM, <i>s</i> -channel ($1s0$ model)	34
3.4.2	Fermion DM, <i>s</i> -channel ($1s\frac{1}{2}$ model)	35
3.4.3	Fermion DM, <i>t</i> -channel ($1t\frac{1}{2}$ model)	38
4	Conclusions	38

1 Introduction

The existence of a Dark Matter (DM) component of the universe is now firmly established, receiving observational support from gravitational effects both on astrophysical scales and on cosmological scales. The DM abundance is precisely known and can be expressed in terms of the critical energy density as $\Omega_{\text{DM}}h^2 = 0.1196 \pm 0.0031$ [1], which corresponds to about one quarter of the total energy content of our universe. Besides this, almost no other experimental information is available about the nature of Dark Matter and its interactions with the Standard Model (SM) of particle physics.

The paradigm for the DM particle which has been most thoroughly studied, especially motivated by the attempts to solve the hierarchy problem such as Supersymmetry, is that of a Weakly Interacting Massive Particles (WIMP), with weak-scale interactions and masses in the range of about GeV-TeV. In this review we will stick to the WIMP paradigm, so we will use DM and WIMP interchangeably.

Experimental searches for WIMPs attack the problem from very different angles, in an attempt to (directly or indirectly) probe the nature of the DM particle. Broadly speaking, the search strategies currently ongoing proceed in three main directions: (1) collider searches, identifying the traces of direct production of DM in particle colliders; (2) direct searches, looking for the scattering events of DM with heavy nuclei in a shielded underground laboratory; (3) indirect searches, detecting the final products of DM annihilations in the galaxy or in the Sun, such as gamma-rays or neutrinos.

The benefit of exploiting the complementary interplay among these different approaches is to improve the discovery potential in a significant way. As this interplay is gaining more and more importance in recent years, the need for a common language into which to translate the results of the different searches has become more pressing. The efforts to develop more model-independent approaches to DM searches (especially for collider physics) stimulated a vast literature on the subject [2–104].

The approach of using Effective Field Theory (EFT) is based on describing the unknown DM interactions with the SM in a very economical way. This has attracted significant attention, especially because of its simplicity and flexibility which allows it to be used in vastly different search contexts. Unfortunately, the validity of this approach, as far as the collider searches for DM are concerned, has been questioned [25, 27, 50, 57, 64, 105] and the limitations to the use of EFTs are by now recognized by the theoretical and experimental communities [106–110].

Certainly, one way out of this *impasse* is to resort to full-fledged models of new physics, comprising a DM candidate. For example, models connected to the solution of the hierarchy problem, such as supersymmetric models or models with a composite Higgs, are already being thoroughly studied. These kinds of searches for DM within more complete frameworks of particle physics have been and are currently the subject of a great deal of research. The results often play the role of benchmarks to be used among different communities of DM hunters. On the other hand, more fundamental frameworks necessarily involve many parameters. Therefore, the inverse problem, i.e. using experimental results to understand the theory space, necessarily involves a large number of degeneracies. This is a particularly severe problem for DM, for which the only precisely known property is the relic abundance.

A “third-way” between these two extremes, the effective-operator approximation and complete ultraviolet models, is possible and is indeed convenient.

The logic behind the so-called *simplified models* [111–113] is to expand the effective-operator interaction to include the degrees of freedom of a “mediator” particle, which connects the DM particle with the Standard Model sector. This amounts to assuming that our “magnifying glass” (the LHC or a future collider) is powerful enough to be able to go beyond the coarse-grained picture provided by EFT and resolve more microscopic – though not all – details which were integrated out. In the limit of sufficiently heavy mediators, the EFT situation is recovered.

This way of proceeding has appealing features as well as limitations. Of course, despite being simple and effective, this is not the only way to go. In fact one may look for alternative scenarios which, while not fully committing to specific models, still offer diversified phenomenology, e.g. along the lines of the benchmarks in Ref. [114]. Furthermore, the simplified model approach may look rather academic, as these models are unlikely to be a realistic fundamental theory.

On the other hand, simplified models retain some of the virtues of the other extreme approaches: a small number of manageable parameters for simpler search strategies, and close contact with ultraviolet completions, which reduce to the simplified models in some particular low-energy limit. Moreover, one can exploit the direct searches for the mediator as a complementary tool to explore the dark sector.

In this review, we summarize the state of the art of DM searches using EFT and simplified models. Our focus will be primarily on collider searches but we will also discuss the connections with direct and indirect searches for DM. In Section 2 we highlight the virtues and drawbacks of the EFT approach, and provide the formulae which are necessary to establish the links among collider/direct/indirect searches, so that a unified picture emerges. In Section 3 we shift the attention to the simplified models. A classification of these mod-

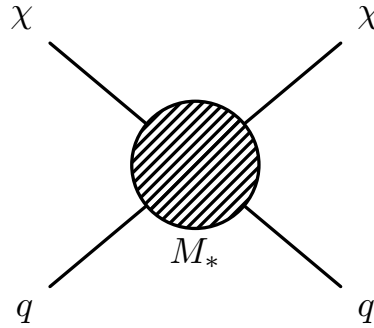


Fig. 1: Schematic of an EFT interaction between DM and the SM

els according to the quantum numbers of the mediator and DM particles and the tree-level mediation channel, is used as a guideline for the discussion of the different kinds of model. We also propose an easy-to-remember nomenclature for the simplified models and point out which ones still need further investigation.

2 Effective Field Theories: virtues and drawbacks

Given that the particle nature of DM and its interactions are still unknown, it is important that analyses of experimental data include constraints that cover as broad a range of DM models as possible in a way that is as model-independent as possible. Whilst the EFT approach does have limitations, it remains a powerful tool to achieve this goal. This approach should be complemented by both limits on the raw signal, and constraints on models which capture the full phenomenology of well-motivated UV-complete DM models, but none of these approaches should stand in isolation.

The EFT approach involves reducing the interactions between DM and the SM fields down to contact interactions, described by a set of non-renormalisable operators, for example,

$$\mathcal{L}_{\text{EFT}} = \frac{1}{M_*^2} (\bar{q}q)(\bar{\chi}\chi). \quad (1)$$

In this case, a fermionic DM particle χ and SM quark q are coupled via a scalar interaction. The strength of the interaction is governed by an energy scale M_* , taken to the appropriate power for this dimension-6 operator

The beauty of the EFT approach is that each operator and energy scale describe a range of processes, depending on the direction of the arrow of time in Fig. 1: DM annihilation, scattering, and production can all be described by the same operator. As we will describe in more detail in the following section, calculations using these operators correspond to taking an expansion in powers of the energy scale of the interaction, along the lines of E^n/M_*^n , and truncating. Therefore EFT calculations are a consistent description of a higher-order process if and only if the energy scale of the interaction is small compared to the energy scale M_* . Therefore the EFT description is strongest when there is a clear separation between the energy scales of the operator and the interaction. In the context of DM searches, there are several situations where the EFT approach is absolutely solid. In indirect searches, for example, the energy scale for the non-relativistic annihilation of DM particles in the halo

Label	Operator	Usual coefficient	Dimension
\mathcal{O}_{D1}	$\bar{\chi}\chi\bar{q}q$	m_q/M_*^3	6
\mathcal{O}_{D2}	$\bar{\chi}i\gamma_5\chi\bar{q}q$	m_q/M_*^3	6
\mathcal{O}_{D3}	$\bar{\chi}\chi\bar{q}i\gamma_5q$	m_q/M_*^3	6
\mathcal{O}_{D4}	$\bar{\chi}i\gamma_5\chi\bar{q}i\gamma_5q$	m_q/M_*^3	6
\mathcal{O}_{D5}	$\bar{\chi}\gamma^\mu\chi\bar{q}\gamma_\mu q$	$1/M_*^2$	6
\mathcal{O}_{D6}	$\bar{\chi}\gamma^\mu\gamma_5\chi\bar{q}\gamma_\mu q$	$1/M_*^2$	6
\mathcal{O}_{D7}	$\bar{\chi}\gamma^\mu\chi\bar{q}\gamma_\mu\gamma_5 q$	$1/M_*^2$	6
\mathcal{O}_{D8}	$\bar{\chi}\gamma^\mu\gamma_5\chi\bar{q}\gamma_\mu\gamma_5 q$	$1/M_*^2$	6
\mathcal{O}_{D9}	$\bar{\chi}\sigma^{\mu\nu}\chi\bar{q}\sigma_{\mu\nu}q$	$1/M_*^2$	6
\mathcal{O}_{D10}	$\bar{\chi}i\sigma^{\mu\nu}\gamma_5\chi\bar{q}\sigma_{\mu\nu}q$	$1/M_*^2$	6
\mathcal{O}_{D11}	$\bar{\chi}\chi G_{\mu\nu}G^{\mu\nu}$	$\alpha_S/4M_*^3$	7
\mathcal{O}_{D12}	$\bar{\chi}\gamma_5\chi G_{\mu\nu}G^{\mu\nu}$	$i\alpha_S/4M_*^3$	7
\mathcal{O}_{D13}	$\bar{\chi}\chi G_{\mu\nu}\tilde{G}^{\mu\nu}$	$\alpha_S/4M_*^3$	7
\mathcal{O}_{D14}	$\bar{\chi}\gamma_5\chi G_{\mu\nu}\tilde{G}^{\mu\nu}$	$i\alpha_S/4M_*^3$	7

Table 1: Operators for Dirac DM.

is of the order of the DM mass m_{DM} ; direct DM searches probe the non-relativistic DM-nucleon operator, where the energy transfer is of the order of MeV. Therefore, as long as the mediator is heavier than $\mathcal{O}(\text{MeV})$ ($\mathcal{O}(m_{\text{DM}})$), EFTs can provide a consistent description of (in)direct detection, as we outline in Sections 2.2 and 2.3.

However, the situation is substantially different in LHC searches for DM. In fact, effective operators are a tool to describe the effects of heavy particles (or ‘mediators’) in the low energy theory where these particles have been integrated out. But the LHC machine delivers scattering events at energies so high, that they may directly produce the mediator itself. Of course, in this case the EFT description fails. While EFT analyses remain a useful tool for LHC searches, this simple point calls for a careful and consistent use of the EFT, checking its range of validity, in the context of DM searches at the LHC.

2.1 Effective Field Theories for collider searches

EFTs are useful at colliders as a parameterisation of missing energy searches. If DM is produced alongside one or more energetic SM particles, then the vector sum of the visible transverse momentum will be non-zero, indicating the presence of particles invisible to the detector, such as neutrinos, DM, or long-lived undetected particles.

The most relevant operators for collider searches are the relativistic DM-quark and DM-gluon operators, shown in Tables 1 and 2 for Dirac and Majorana fermionic DM, and Tables 3 and 4 for complex and real scalar DM respectively, where $\tilde{G}^{\mu\nu} \equiv \epsilon^{\mu\nu\rho\sigma} G_{\rho\sigma}$. The parameter M_* is of course independent for each operator, and in principle for each flavor of quark, although M_* is generally assumed to be flavor-universal in collider studies, in order to avoid issues with flavor constraints, such as flavor-changing neutral currents.

Label	Operator	Usual coefficient	Dimension
\mathcal{O}_{M1}	$\bar{\chi}\chi\bar{q}q$	$m_q/2M_*^3$	6
\mathcal{O}_{M2}	$\bar{\chi}i\gamma_5\chi\bar{q}q$	$m_q/2M_*^3$	6
\mathcal{O}_{M3}	$\bar{\chi}\chi\bar{q}i\gamma_5q$	$m_q/2M_*^3$	6
\mathcal{O}_{M4}	$\bar{\chi}i\gamma_5\chi\bar{q}i\gamma_5q$	$m_q/2M_*^3$	6
\mathcal{O}_{M5}	$\bar{\chi}\gamma^\mu\gamma_5\chi\bar{q}\gamma_\mu\gamma_5q$	$1/2M_*^2$	6
\mathcal{O}_{M6}	$\bar{\chi}\gamma^\mu\gamma_5\chi\bar{q}\gamma_\mu\gamma_5q$	$1/2M_*^2$	6
\mathcal{O}_{M7}	$\bar{\chi}\chi G_{\mu\nu}G^{\mu\nu}$	$\alpha_S/8M_*^3$	7
\mathcal{O}_{M8}	$\bar{\chi}\gamma_5\chi G_{\mu\nu}G^{\mu\nu}$	$i\alpha_S/8M_*^3$	7
\mathcal{O}_{M9}	$\bar{\chi}\chi G_{\mu\nu}\tilde{G}^{\mu\nu}$	$\alpha_S/8M_*^3$	7
\mathcal{O}_{M10}	$\bar{\chi}\gamma_5\chi G_{\mu\nu}\tilde{G}^{\mu\nu}$	$i\alpha_S/8M_*^3$	7

Table 2: Operators for Majorana DM.

Label	Operator	Usual coefficient	Dimension
\mathcal{O}_{C1}	$\phi^*\phi\bar{q}q$	m_q/M_*^2	5
\mathcal{O}_{C2}	$\phi^*\phi\bar{q}i\gamma_5q$	m_q/M_*^2	5
\mathcal{O}_{C3}	$\phi^*i\overset{\leftrightarrow}{\partial}_\mu\phi\bar{q}\gamma^\mu q$	$1/M_*^2$	6
\mathcal{O}_{C4}	$\phi^*i\partial_\mu\phi\bar{q}\gamma^\mu\gamma_5q$	$1/M_*^2$	6
\mathcal{O}_{C5}	$\phi^*\phi G_{\mu\nu}G^{\mu\nu}$	$\alpha_S/4M_*^2$	6
\mathcal{O}_{C6}	$\phi^*\phi G_{\mu\nu}\tilde{G}^{\mu\nu}$	$\alpha_S/4M_*^2$	6

Table 3: Operators for Complex Scalar DM.

Label	Operator	Usual coefficient	Dimension
\mathcal{O}_{R1}	$\phi^2\bar{q}q$	$m_q/2M_*^2$	5
\mathcal{O}_{R2}	$\phi^2\bar{q}i\gamma_5q$	$m_q/2M_*^2$	5
\mathcal{O}_{R3}	$\phi^2G_{\mu\nu}G^{\mu\nu}$	$\alpha_S/8M_*^2$	6
\mathcal{O}_{R4}	$\phi^2G_{\mu\nu}\tilde{G}^{\mu\nu}$	$\alpha_S/8M_*^2$	6

Table 4: Operators for Real Scalar DM.

Generically, EFTs are a valid description of DM interactions with the Standard Model if the interactions are mediated by a heavy particle out of the kinematic reach of the collider. At the energy scales and coupling strengths accessible to the LHC, the validity of the EFT approximation can no longer be guaranteed.

As an illustration of the range of validity of EFT operators, we begin with a benchmark simplified model, where a pair of Dirac DM fermions interact with the SM via *s*-channel

exchange of a Z' -like mediator with pure vector couplings

$$\mathcal{L}_{\text{int}} \supset -Z'_\mu \left(\sum_q g_q \bar{q} \gamma^\mu q + g_\chi \bar{\chi} \gamma^\mu \chi \right). \quad (2)$$

which is going to be discussed in detail in Sect. 3.4.2. The mediator has mass M_{med} and vector couplings to quarks and DM with strength g_q and g_χ respectively, and this model reduces to the \mathcal{O}_{D5} operator in the full EFT limit. At low energies, much smaller than M_{med} , the heavy mediator can be integrated out and one is left with a theory without the mediator, where the interactions between DM and quarks are described by a tower of effective operators. The expansion in terms of this tower can be viewed as the expansion of the propagator of the mediator particle,

$$\frac{g_q g_\chi}{M_{\text{med}}^2 - Q_{\text{tr}}^2} = \frac{g_q g_\chi}{M_{\text{med}}^2} \left(1 + \frac{Q_{\text{tr}}^2}{M_{\text{med}}^2} + \mathcal{O} \left(\frac{Q_{\text{tr}}^4}{M_{\text{med}}^4} \right) \right), \quad (3)$$

where Q_{tr} is the transfer momentum of the process. Retaining only the leading term $1/M_{\text{med}}^2$ corresponds to truncating the expansion to the lowest-dimensional operator. The parameters of the high-energy theory and the scale M_* associated with the dimension-6 operators of the low-energy EFT are then connected via

$$M_* = \frac{M_{\text{med}}}{\sqrt{g_q g_\chi}}, \quad (4)$$

which holds as long as

$$Q_{\text{tr}} \ll M_{\text{med}}. \quad (5)$$

In such an s -channel model, there is a condition defining the point where the approximation has inevitably broken down. The mediator must carry at least enough energy to produce DM at rest, therefore $Q_{\text{tr}} > 2m_{\text{DM}}$. Combining this with Eqs. (4)-(5), we see

$$M_* > \frac{Q_{\text{tr}}}{\sqrt{g_q g_\chi}} > 2 \frac{m_{\text{DM}}}{\sqrt{g_q g_\chi}}, \quad (6)$$

which in the extreme case in which couplings are as large as possible while remaining in the perturbative regime, $g_\chi, g_q < 4\pi$, gives

$$M_* > \frac{m_{\text{DM}}}{2\pi}. \quad (7)$$

Note that this condition is necessary but not sufficient for the validity of the EFT approximation. A better measure of the validity comes from drawing a comparison between Q_{tr} and M_{med} , which defines three regions [57]:

1. When $Q_{\text{tr}}^2 < M_{\text{med}}^2 \equiv g_q g_\chi M_*^2$, the approximation in Eq. (3) holds. This is clearly the only region where the EFT approximation remains valid.
2. In the region where $Q_{\text{tr}}^2 \sim M_{\text{med}}^2$ the production cross-section undergoes a resonant enhancement. The EFT approximation misses this enhancement, and is therefore conservative relative to the full theory.
3. When $Q_{\text{tr}}^2 \gg M_{\text{med}}^2$, the expansion in Eq. (3) fails and the signal cross section falls like Q_{tr}^{-1} rather than M_{med}^{-1} . In this region the EFT constraints will be stronger than the actual ones.

Ref. [109] has calculated the kinematic distribution of events at 14 TeV for both this benchmark simplified model at a range of mediator masses, and the \mathcal{O}_{D5} operator. They find that the spectra become equivalent at a mediator mass of 10 TeV, and so EFTs can be considered a valid description of simplified models with mediators at or above this mass scale. At such large mediator mass scales, it is possible that a constraint on M_* will correspond to very large values of $g_\chi g_q$ above the range where perturbative calculations are valid. In this case it remains problematic to draw a clear correspondence between a constraint on M_* and a constraint on simplified model parameters.

EFTs do not aim to capture the complex physics described by UV-complete models, and so gauge invariance is often not enforced. This can lead to issues if the phenomenology of the operator no longer describes that of a UV complete operator but rather is symptomatic of the violation of gauge invariance. As an example, both ATLAS and CMS have included searches [94, 98, 100] for a version of \mathcal{O}_{D5} where the relative coupling strength to up and down quarks was allowed to vary, leading to an enhancement of the cross section. Ref. [90] pointed out that this enhancement is due to the breaking of gauge invariance. In UV complete models that satisfy gauge invariance, the enhancement is much smaller [115, 116].

Another issue that may arise when dealing with high-energy collisions is to make sure that unitarity of the S-matrix is not violated. When adopting an EFT description, this means that the condition of unitarity preservation sets an energy scale above which the contact interaction is not reliable anymore and a UV completion of the operator must be adopted instead. For instance, for the operator \mathcal{O}_{D5} , the unitarity constraint gives [27]

$$M_* > \left[\left(1 - \frac{4m_\chi^2}{s} \right) s \frac{\sqrt{3}}{4\pi} \right]^{1/2}, \quad (8)$$

where \sqrt{s} is center-of-mass energy of the initial state of the process $q\bar{q} \rightarrow \chi\bar{\chi} + j$ (see Ref. [117] for the constraints on other operators). As a consistency check, the limits on M_* derived experimentally according with any of the two methods described below need to be compared with the unitarity bound.

EFT truncation by comparison with a simplified model. We see from Eqs. (3)-(4) that the validity of the EFT approximation as a description of some UV-complete model depends on the unknown parameters of that model. By introducing a minimum set of free parameters from such a model, one can enforce EFT validity by restricting the signal so that only events which pass the EFT validity condition Eq. (5) are used, thereby removing events for which the high-mediator-mass approximation made in the EFT limit is not a valid approximation in a given model. In a typical s -channel model this EFT validity condition is

$$Q_{tr}^2 < M_{med}^2 = g_q g_\chi M_*^2. \quad (9)$$

Discarding events which do not pass this condition gives a truncated signal cross section as a function of $(m_\chi, g_q g_\chi, M_*)$ or (m_χ, M_{med}) . This can be solved to find a rescaled, conservative limit on the energy scale, M_*^{rescaled} .

Note that if $g_q g_\chi$ is fixed rather than M_{med} , then the truncated cross-section which is used to derive a rescaled limit M_*^{rescaled} is itself a function of the M_*^{rescaled} . Therefore the M_*^{rescaled} is found via a scan or iterative procedure. ATLAS has applied this procedure for a range of operators in Ref. [102].

If instead M_{med} is fixed, then $g_q g_\chi$ must increase to match the new value of M_* via the relation in Eq. (4). If a very large value of M_{med} is chosen or assumed in order to guarantee $Q_{tr}^2 < M_{med}^2$, then the derived constraint on M_* may give a large value of $g_q g_\chi$. If $g_q g_\chi$

becomes sufficiently large, then perturbation theory is no longer a reliable computation technique.

EFT truncation using the center of mass energy. The procedure described above implicitly assumes some kind of knowledge of the underlying UV completion of the EFT. The truncation method relies on the transferred momentum Q_{tr} of the process of interest.

Alternatively, it is possible to extract limits without explicit assumptions about the UV completion, basing the truncation upon the center of mass energy E_{cm} of the process of DM production [118, 119]. The results will be more model-independent, but necessarily weaker than those based on the previous truncation method.

According to this method, the EFT approximation is reliable as long as

$$E_{\text{cm}} < M_{\text{cut}}, \quad (10)$$

where the cutoff scale M_{cut} is what defines the range of validity of the EFT approximation. Such scale can be related to the suppression scale M_* of the effective operator by $M_{\text{cut}} = g_* M_*$, where g_* plays the role of an effective coupling, inherited by an unknown UV completion. For instance, in the case of a UV completion of the type Z' -type model of Eq. 2, one has $g_* = \sqrt{g_\chi g_q}$.

As said, the parameter M_{cut} is associated to the failure of the EFT description and it can be identified by using a ratio R , defined as the fraction of events satisfying the condition $\hat{s} < M_{\text{cut}}^2$. Large enough M_{cut} means all events are retained, so $R = 1$. Small enough M_{cut} means all events are rejected, so $R = 0$, which means no result can be extracted. A useful methodology is to find the values of M_{cut} for which the truncation provides values of R within 0.1 and 1, and then show the corresponding limits for such values of M_{cut} .

If a specific UV completion of the EFT is assumed (or hinted by experiments), the parameters M_{cut} , M_* can be computed in terms of the parameters of the simplified model and the resulting bounds will be more conservative than those obtained by using Q_{tr} . However, if no UV completion is known or assumed, the method described here becomes particularly helpful.

In Ref. [120] the reader can find the details of an explicit application of these two truncation techniques.

2.2 Effective Field Theories for direct detection

Direct detection experiments search for the signature of DM scattering with a terrestrial target. Currently the most sensitive experiments use a noble liquid target material in a two-phase time projection chamber. This design allows the experiment to see two signals: the prompt photons from scintillation events, and a delayed signal from ionisation events. The ratio between these two signals allows the experiment to distinguish between nuclear and electronic recoils, reducing the background from scattering due to cosmic rays and background radiation. This gives a constraint on the energy spectrum of DM-nucleus recoil events dR/dE_R , which is in turn used to constrain the DM-nucleon scattering cross-section via the relation (per unit target mass)

$$\frac{dR}{dE_R} = \frac{\rho_\chi}{m_\chi m_N} \int_{|\mathbf{v}| > v_{\text{min}}} d^3\mathbf{v} |\mathbf{v}| f(\mathbf{v}) \frac{d\sigma_{\chi A}}{dE_R}, \quad (11)$$

where ρ_χ is the local DM density, $v_{\min} = \sqrt{m_A E_R^{\text{th}} / (2\mu_{\chi A})^2}$ is the minimum DM velocity required to transfer a threshold recoil kinetic energy E_R^{th} to the nucleus A , $\mu_{\chi A}$ is the DM-nucleus reduced mass, $f(\mathbf{v})$ is the local DM velocity distribution, and $d\sigma_{\chi A}/dE_R$ is the differential DM-nucleus scattering cross section. The energy dependence of $d\sigma_{\chi A}/dE_R$ for a given detector depends on the underlying DM model and contains a nuclear form factor. This cross section can be computed starting from a more basic quantity, the DM-nucleon scattering cross section at zero momentum transfer $\sigma_{\chi N}$ (with $N = n, p$) which is the quantity commonly constrained by the experimental collaborations and can be thought of as the normalisation of the full cross-section $d\sigma_{\chi A}/dE_R$.

The scattering interactions involved in direct detection experiments are at a vastly different energy scale than those at the LHC. In a DM-nucleon scattering event, the DM velocity is of order $10^{-3}c$ and the momentum transfer is only $\mathcal{O}(10\text{ MeV})$ [10], which leads to two main differences when compared with the picture at colliders: (1) in direct detection experiments, the EFT approximations will be valid for a much larger range of parameters (DM masses, coupling strengths, etc.); and (2) the relevant operators are not the usual DM-parton operators considered in Section 2.1, but rather the non-relativistic limit of DM-nucleon operators. A partial list of these operators is given in Table 5, in the language of [32, 121]. The large splitting between the LHC and direct detection energy scales makes it important to remember that the operator coefficients need to be RG-evolved from the high energy theory, including the matching conditions at the quark masses thresholds [89, 122].

The matrix element describing DM-nucleon contact interactions is then given by a sum of the contributions from each non-relativistic operator

$$\mathcal{M} = \sum_{i=1}^{12} c_i^N(m_\chi) \mathcal{O}_i^{\text{NR}}. \quad (12)$$

Next we show how to translate between the language of relativistic DM-quark operators discussed in Section 2.1 and direct detection constraints on the non-relativistic DM-nucleon operators in Table 5 [10, 32, 121].

To do this, first we consider the intermediate-stage relativistic DM-nucleon operators, beginning with the Dirac DM listed in Table 6 as a concrete example, with other cases discussed later. The effective Lagrangian at nucleon level gains contributions from DM interactions with quarks and gluons and can be written at either level as

$$\mathcal{L}_{\text{eff}} = \sum_{q,i} c_i^q \mathcal{O}_i^q + \sum_{g,j} c_j^g \mathcal{O}_j^g = \sum_{N,k} c_k^N \mathcal{O}_k^N, \quad (13)$$

where i, j are summed over whichever operators are present in the model of interest, and $N = n, p$. This will induce a sum over some subset k of nucleonic operators. The value of the coefficients c_k^N , given in the third column of Table 6, are a function of the coefficients of the DM-quark and DM-gluon operators, c_i^q and c_j^g . These are dimensionful coefficients, with the usual parameterisation given in the third column of Table 1 for Dirac DM.

The coefficients c_k^N in Table 6 are also a function of several other parameters. Note that $f_G^{(N)} \equiv 1 - \sum_{q=u,d,s} f_q^{(N)}$, and $C_{3,4} = \left(\sum_q c_{3,4}^q / m_q \right) \left(\sum_{q=u,d,s} m_q^{-1} \right)^{-1}$. There is some uncertainty in the determination of $f_q^{(N)}$, $\delta_q^{(N)}$ and $\Delta_q^{(N)}$. As a benchmark, we show the values used by `micrOMEGAs` [123] in Table 7. Notice that other sets of values are also available in the literature, see Refs. [124–128] for $f_q^{(N)}$, $\Delta_q^{(N)}$ and Refs. [129, 130] and Ref. [131] for other determinations of $\delta_q^{(N)}$.

Label	Operator
$\mathcal{O}_1^{\text{NR}}$	\not{p}
$\mathcal{O}_3^{\text{NR}}$	$i\mathbf{s}_N \cdot (\mathbf{q} \times \mathbf{v}^\perp)$
$\mathcal{O}_4^{\text{NR}}$	$\mathbf{s}_\chi \cdot \mathbf{s}_N$
$\mathcal{O}_5^{\text{NR}}$	$i\mathbf{s}_\chi \cdot (\mathbf{q} \times \mathbf{v}^\perp)$
$\mathcal{O}_6^{\text{NR}}$	$(\mathbf{s}_\chi \cdot \mathbf{q})(\mathbf{s}_N \cdot \mathbf{q})$
$\mathcal{O}_7^{\text{NR}}$	$\mathbf{s}_N \cdot \mathbf{v}^\perp$
$\mathcal{O}_8^{\text{NR}}$	$\mathbf{s}_\chi \cdot \mathbf{v}^\perp$
$\mathcal{O}_9^{\text{NR}}$	$i\mathbf{s}_\chi \cdot (\mathbf{s}_N \times \mathbf{q})$
$\mathcal{O}_{10}^{\text{NR}}$	$i\mathbf{s}_N \cdot \mathbf{q}$
$\mathcal{O}_{11}^{\text{NR}}$	$i\mathbf{s}_\chi \cdot \mathbf{q}$
$\mathcal{O}_{12}^{\text{NR}}$	$\mathbf{v}^\perp \cdot (\mathbf{s}_\chi \times \mathbf{s}_N)$

Table 5: Non-relativistic DM-nucleon contact operators relevant to describing the interactions listed in Section 2.1. The operator $\mathcal{O}_2^{\text{NR}} = (\mathbf{v}^\perp)^2$ from Ref. [32] is not induced by any of the relativistic operators considered in Sec. 2.1 and so is not discussed here.

Label	Operator	DM-parton coefficient c_k^N
$\mathcal{O}_{\text{D}1}^{\text{N}}$	$\bar{\chi}\chi\bar{N}N$	$\sum_{q=u,d,s} c_{\text{D}1}^q \frac{m_N}{m_q} f_q^{(N)} + \frac{2}{27} f_G^{(N)} (\sum_{q=c,b,t} c_{\text{D}1}^q \frac{m_N}{m_q} - \frac{1}{3\pi} c_{\text{D}11}^g m_N)$
$\mathcal{O}_{\text{D}2}^{\text{N}}$	$\bar{\chi}i\gamma_5\chi\bar{N}N$	$\sum_{q=u,d,s} c_{\text{D}2}^q \frac{m_N}{m_q} f_q^{(N)} + \frac{2}{27} f_G^{(N)} (\sum_{q=c,b,t} c_{\text{D}2}^q \frac{m_N}{m_q} - \frac{1}{3\pi} c_{\text{D}12}^g m_N)$
$\mathcal{O}_{\text{D}3}^{\text{N}}$	$\bar{\chi}\chi\bar{N}i\gamma_5N$	$\sum_{q=u,d,s} \frac{m_N}{m_q} [(c_{\text{D}3}^q - C_3) + \frac{1}{2\pi} c_{\text{D}13}^g \bar{m}] \Delta_q^{(N)}$
$\mathcal{O}_{\text{D}4}^{\text{N}}$	$\bar{\chi}i\gamma_5\chi\bar{N}i\gamma_5N$	$\sum_{q=u,d,s} \frac{m_N}{m_q} [(c_{\text{D}4}^q - C_4) + \frac{1}{2\pi} c_{\text{D}14}^g \bar{m}] \Delta_q^{(N)}$
$\mathcal{O}_{\text{D}5}^{\text{N}}$	$\bar{\chi}\gamma^\mu\chi\bar{N}\gamma_\mu N$	$2c_{\text{D}5}^u + c_{\text{D}5}^d$ for $\mathcal{O}_{\text{D}5}^{\text{P}}$, and $c_{\text{D}5}^u + 2c_{\text{D}5}^d$ for $\mathcal{O}_{\text{D}5}^{\text{n}}$
$\mathcal{O}_{\text{D}6}^{\text{N}}$	$\bar{\chi}\gamma^\mu\gamma_5\chi\bar{N}\gamma_\mu N$	$2c_{\text{D}6}^u + c_{\text{D}6}^d$ for $\mathcal{O}_{\text{D}6}^{\text{P}}$, and $c_{\text{D}6}^u + 2c_{\text{D}6}^d$ for $\mathcal{O}_{\text{D}6}^{\text{n}}$
$\mathcal{O}_{\text{D}7}^{\text{N}}$	$\bar{\chi}\gamma^\mu\chi\bar{N}\gamma_\mu\gamma_5 N$	$\sum_q c_{\text{D}7}^q \Delta_q^{(N)}$
$\mathcal{O}_{\text{D}8}^{\text{N}}$	$\bar{\chi}\gamma^\mu\gamma_5\chi\bar{N}\gamma_\mu\gamma_5 N$	$\sum_q c_{\text{D}8}^q \Delta_q^{(N)}$
$\mathcal{O}_{\text{D}9}^{\text{N}}$	$\bar{\chi}\sigma^{\mu\nu}\chi\bar{N}\sigma_{\mu\nu} N$	$\sum_q c_{\text{D}9}^q \delta_q^{(N)}$
$\mathcal{O}_{\text{D}10}^{\text{N}}$	$\bar{\chi}i\sigma^{\mu\nu}\gamma_5\chi\bar{N}\sigma_{\mu\nu} N$	$\sum_q c_{\text{D}10}^q \delta_q^{(N)}$

Table 6: DM-nucleon operators for Dirac fermion DM. For Majorana DM, $\mathcal{O}_{\text{D}5}$, $\mathcal{O}_{\text{D}7}$, $\mathcal{O}_{\text{D}9}$ and $\mathcal{O}_{\text{D}10}$ disappear. The coefficients $c_{\text{D}1 \dots \text{D}10}^q$, $c_{\text{D}11 \dots \text{D}13}^g$ are the corresponding coefficients from the third column of Table 1, e.g. $c_{\text{D}5}^q = 1/M_*^2$. Recall that the coefficients are in principle independent for each quark flavor.

$f_u^{(p)}$	$f_d^{(p)}$	$f_s^{(p)}$	$\Delta_u^{(p)}$	$\Delta_d^{(p)}$	$\Delta_s^{(p)}$	$\delta_u^{(p)}$	$\delta_d^{(p)}$	$\delta_s^{(p)}$
0.0153	0.0191	0.0447	0.842	-0.427	-0.085	0.84	-0.23	-0.046
$f_u^{(n)}$	$f_d^{(n)}$	$f_s^{(n)}$	$\Delta_u^{(n)}$	$\Delta_d^{(n)}$	$\Delta_s^{(n)}$	$\delta_u^{(n)}$	$\delta_d^{(n)}$	$\delta_s^{(n)}$
0.011	0.0273	0.0447	-0.427	0.842	-0.085	-0.23	0.84	-0.046

Table 7: Quark-nucleon form factors as used by `micrOMEGAs` [123]. Note that $f_s^{(p)} = f_s^{(n)}$, $\Delta_u^{(p)} = \Delta_d^{(n)}$, $\Delta_d^{(p)} = \Delta_u^{(n)}$, etc.

The next step is to establish relationships between relativistic and non-relativistic operators. At leading order in the non-relativistic limit, the DM-nucleon operators in Table 6 reduce down to a combination of the operators from Table 5 according to the relations

$$\begin{aligned}
\langle \mathcal{O}_{D1}^N \rangle &= \langle \mathcal{O}_{D5}^N \rangle = 4m_\chi m_N \mathcal{O}_1^{\text{NR}}, \\
\langle \mathcal{O}_{D2}^N \rangle &= -4m_N \mathcal{O}_{11}^{\text{NR}}, \\
\langle \mathcal{O}_{D3}^N \rangle &= 4m_\chi \mathcal{O}_{10}^{\text{NR}}, \\
\langle \mathcal{O}_{D4}^N \rangle &= 4\mathcal{O}_6^{\text{NR}}, \\
\langle \mathcal{O}_{D6}^N \rangle &= 8m_\chi (m_N \mathcal{O}_8^{\text{NR}} + \mathcal{O}_9^{\text{NR}}), \\
\langle \mathcal{O}_{D7}^N \rangle &= 8m_N (-m_\chi \mathcal{O}_8^{\text{NR}} + \mathcal{O}_9^{\text{NR}}), \\
\langle \mathcal{O}_{D8}^N \rangle &= -\frac{1}{2} \langle \mathcal{O}_{D9}^N \rangle = -16m_\chi m_N \mathcal{O}_4^{\text{NR}}, \\
\langle \mathcal{O}_{D10}^N \rangle &= 8(m_\chi \mathcal{O}_{11}^{\text{NR}} - m_N \mathcal{O}_{10}^{\text{NR}} - 4m_\chi m_N \mathcal{O}_{12}^{\text{NR}}). \tag{14}
\end{aligned}$$

Using these relationships, the matrix-element for the interactions described by the Lagrangian in Eq. (13) can be rewritten in terms of a sum of non-relativistic operators. Used in combination with Eq. (12), the coefficients c_i^N of the NR operators can be converted into those of the relativistic operators and vice-versa.

As an example, let us consider the \mathcal{O}_{D5} operator. If the coupling to each flavor of quark is chosen to be independent, i.e. $c_{D1}^q = 1/M_{*,q}^2$, then the effective Lagrangian at the DM-quark level is

$$\mathcal{L}_{\text{eff}} = \sum_q c_{D5}^q \mathcal{O}_{D5}^q = \sum_q \frac{1}{M_{*,q}^2} \bar{\chi} \gamma^\mu \chi \bar{q} \gamma_\mu q. \tag{15}$$

Combining this with the information in Table 6, we see that this operator contributes to \mathcal{O}_{D5}^N , and so the effective Lagrangian at DM-nucleon level is

$$\begin{aligned}
\mathcal{L}_{\text{eff}} &= \sum_N c_{D5}^N \mathcal{O}_{D5}^N = (2c_{D5}^u + c_{D5}^n) \mathcal{O}_{D5}^p + (c_{D5}^u + 2c_{D5}^n) \mathcal{O}_{D5}^n \\
&= \left(\frac{2}{M_{*,u}^2} + \frac{1}{M_{*,d}^2} \right) \bar{\chi} \gamma^\mu \chi \bar{p} \gamma_\mu p + \left(\frac{1}{M_{*,u}^2} + \frac{2}{M_{*,d}^2} \right) \bar{\chi} \gamma^\mu \chi \bar{n} \gamma_\mu n. \tag{16}
\end{aligned}$$

Label	Operator	DM-parton coefficient c_k^N
\mathcal{O}_{C1}^N	$\phi^* \phi \bar{N} N$	$\sum_{q=u,d,s} c_{C1}^q \frac{m_N}{m_q} f_q^{(N)} + \frac{2}{27} f_G^{(N)} (\sum_{q=c,b,t} c_{C1}^q \frac{m_N}{m_q} - \frac{1}{3\pi} c_{C5}^g m_N)$
\mathcal{O}_{C2}^N	$\phi^* \phi \bar{N} i \gamma_5 N$	$\sum_{q=u,d,s} \frac{m_N}{m_q} [(c_{C2}^q - C_2) + \frac{1}{2\pi} c_{C6}^g \tilde{m}] \Delta_q^{(N)}$
\mathcal{O}_{C3}^N	$\phi^* i \overleftrightarrow{\partial}_\mu \phi \bar{N} \gamma^\mu N$	$2c_{C3}^u + c_{C3}^d$ for \mathcal{O}_{C3}^p , and $c_{C3}^u + 2c_{C3}^d$ for \mathcal{O}_{C3}^n
\mathcal{O}_{C4}^N	$\phi^* i \overleftrightarrow{\partial}_\mu \phi \bar{N} \gamma^\mu \gamma_5 N$	$\sum_q c_{C4}^q \Delta_q^{(N)}$

Table 8: DM-nucleon operators for complex scalar fermion DM.

Using Eq. (14), we see that $\langle \mathcal{O}_{D5}^N \rangle = 4m_\chi m_N \mathcal{O}_1^{\text{NR}}$, therefore the matrix element is

$$\begin{aligned} \mathcal{M} &= \sum_N c_{D5}^N \langle \mathcal{O}_{D5}^N \rangle \\ &= \left[4m_\chi m_p \left(\frac{2}{M_{*,u}^2} + \frac{1}{M_{*,d}^2} \right) + 4m_\chi m_n \left(\frac{1}{M_{*,u}^2} + \frac{2}{M_{*,d}^2} \right) \right] \mathcal{O}_1^{\text{NR}} \\ &= (\mathfrak{c}_1^p(m_\chi) + \mathfrak{c}_1^n(m_\chi)) \mathcal{O}_1^{\text{NR}} \end{aligned} \quad (17)$$

Ref. [121] provides a toolset to convert experimental data into a constraint on any combination of relativistic or non-relativistic operators, by defining a benchmark constraint on an arbitrary operator and using the conversion formula

$$\mathfrak{c}_i^p(m_\chi)^2 = \sum_{i,j=1}^{12} \sum_{N,N'=p,n} \mathfrak{c}_i^N(m_\chi) \mathfrak{c}_j^{N'}(m_\chi) \mathcal{Y}_{i,j}^{(N,N')}(m_\chi) \quad (18)$$

where $\mathcal{Y}_{i,j}^{(N,N')}$ are given as a set of interpolating functions for each experiment.

To reiterate, in this section we have summarised how to convert between the coefficients $\mathfrak{c}_i^N(m_\chi)$ of the NR operators relevant for direct detection, and the coefficients c_i^q or M_* of the fundamental underlying DM-parton operators. With this information, Eq. (18) can be used to convert between constraints on different operators using e.g. the code given in Ref. [121].

Moving beyond Dirac DM, the relationships between operators for Majorana DM are very similar to those given in Table 6, the difference being that \mathcal{O}_{D5} , \mathcal{O}_{D7} , \mathcal{O}_{D9} and \mathcal{O}_{D10} disappear and so do not have a Majorana analogue. Therefore \mathcal{O}_{D5}^N , \mathcal{O}_{D7}^N also do not have a Majorana version.

For complex scalar DM, the DM-nucleon operators are given in Table 8. At leading order in the non-relativistic limit, these reduce to

$$\begin{aligned} \langle \mathcal{O}_{C1}^N \rangle &= 2m_N \mathcal{O}_1^{\text{NR}}, \\ \langle \mathcal{O}_{C2}^N \rangle &= 2\mathcal{O}_{10}^{\text{NR}}, \\ \langle \mathcal{O}_{C3}^N \rangle &= 4m_\chi m_N \mathcal{O}_1^{\text{NR}}, \\ \langle \mathcal{O}_{C4}^N \rangle &= -8m_\chi m_N \mathcal{O}_7^{\text{NR}}. \end{aligned} \quad (19)$$

For real scalar DM, $\phi^* \equiv \phi$ and \mathcal{O}_{C3}^N , \mathcal{O}_{C4}^N vanish.

The final step to make contact with experimental results is to draw a relationship between the coefficients of the DM-parton operators and the notation used in the direct detection community, where constraints on the scattering rate are usually given in terms of either

spin-independent scattering cross section σ_{SI} , or the spin-dependent scattering cross section σ_{SD} . These two parameterisations of the scattering rate are induced by the lowest-order expansion of specific non-relativistic operators.

The spin-independent scattering rate corresponds to a constraint on c_i^N of $\mathcal{O}_1^{\text{NR}}$. This operator is the only one not suppressed by either the momentum of the DM or a spin coupling, and so is the most commonly studied interaction in the community.

The spin-dependent rate σ_{SD} corresponds to a constraint on c_i^N of $\mathcal{O}_4^{\text{NR}}$. This corresponds to an interaction of the DM spin with the nuclear spin and therefore the scattering rate is suppressed by the spin of the target nucleus. Not all experiments are sensitive to this interaction.

From Eqs. (14) and (19) we see that several DM-nucleon operators lead to these two NR operators. Specifically: $\mathcal{O}_{\text{D}1}^{\text{N}}$, $\mathcal{O}_{\text{D}5}^{\text{N}}$, $\mathcal{O}_{\text{C}1}^{\text{N}}$, and $\mathcal{O}_{\text{C}3}^{\text{N}}$ lead to $\mathcal{O}_1^{\text{NR}}$, while $\mathcal{O}_{\text{D}8}^{\text{N}}$, $\mathcal{O}_{\text{D}9}^{\text{N}}$ lead to $\mathcal{O}_4^{\text{NR}}$. At the DM-quark level, $\mathcal{O}_{\text{D}1}$, $\mathcal{O}_{\text{D}5}$, $\mathcal{O}_{\text{D}11}$, $\mathcal{O}_{\text{C}1}$, $\mathcal{O}_{\text{C}3}$ and $\mathcal{O}_{\text{C}5}$ each lead to a spin-independent scattering cross section, while $\mathcal{O}_{\text{D}8}$, $\mathcal{O}_{\text{D}9}$ lead to a spin-dependent scattering cross section. The formula for σ_{SI} , σ_{SD} for each of these operators \mathcal{O}_i is

$$\sigma_{\text{SI}} = \frac{\mu_{\chi N}^2}{\pi} (c_i^N)^2, \quad (20)$$

$$\sigma_{\text{SD}} = \frac{3\mu_{\chi N}^2}{\pi} (c_i^N)^2, \quad (21)$$

where c_i^N is given in Table 6 for Dirac fermion DM and Table 8 for complex scalar DM, $\mu_{\chi N} = m_\chi m_N / (m_\chi + m_N)$ is the DM-nucleon reduced mass, and the target nucleon is either a neutron or a proton $N = n, p$.

The precise application of these formulae to convert between σ_{SI} , σ_{SD} and the usual coefficients c_i^q from Tables 1, 3 is sensitive to the choice of the nuclear form factors (see Table 7), and so we list here the usual conversion used by the community [11],

$$\sigma_{\text{SI}}^{\text{D}1} = 1.60 \times 10^{-37} \text{ cm}^2 \left(\frac{\mu_{\chi N}}{1 \text{ GeV}} \right)^2 \left(\frac{20 \text{ GeV}}{M_*} \right)^6 \quad (22)$$

$$\sigma_{\text{SI}}^{\text{D}5, \text{C}3} = 1.38 \times 10^{-37} \text{ cm}^2 \left(\frac{\mu_{\chi N}}{1 \text{ GeV}} \right)^2 \left(\frac{300 \text{ GeV}}{M_*} \right)^4 \quad (23)$$

$$\sigma_{\text{SI}}^{\text{D}11} = 3.83 \times 10^{-41} \text{ cm}^2 \left(\frac{\mu_{\chi N}}{1 \text{ GeV}} \right)^2 \left(\frac{100 \text{ GeV}}{M_*} \right)^6 \quad (24)$$

$$\sigma_{\text{SI}}^{\text{C}1} = 2.56 \times 10^{-36} \text{ cm}^2 \left(\frac{\mu_{\chi N}}{1 \text{ GeV}} \right)^2 \left(\frac{10 \text{ GeV}}{M_*} \right)^4 \left(\frac{10 \text{ GeV}}{m_\chi} \right)^2 \quad (25)$$

$$\sigma_{\text{SI}}^{\text{C}5} = 7.40 \times 10^{-39} \text{ cm}^2 \left(\frac{\mu_{\chi N}}{1 \text{ GeV}} \right)^2 \left(\frac{60 \text{ GeV}}{M_*} \right)^4 \left(\frac{10 \text{ GeV}}{m_\chi} \right)^2 \quad (26)$$

$$\sigma_{\text{SD}}^{\text{D}8, \text{D}9} = 4.70 \times 10^{-39} \text{ cm}^2 \left(\frac{\mu_{\chi N}}{1 \text{ GeV}} \right)^2 \left(\frac{300 \text{ GeV}}{M_*} \right)^4. \quad (27)$$

It is possible to convert constraints on σ_{SI} and σ_{SD} into constraints on the parameters of any other operator or combination of operators using Eq. (18) with the code described in Ref. [121].

2.3 Effective Field Theories for indirect detection

Indirect detection is the search for the Standard Model particles arising as a result of DM self-annihilations (see e.g. Ref. [132] for a state-of-the-art review). DM annihilation takes place on many scales, from cosmological scales down to annihilation within the solar system.

Most indirect detection studies search for the gamma-ray signal from WIMP annihilation on the scale of Galactic halos. Both direct production of photons and secondary production from the decay of other SM particles are considered. For annihilation of DM of mass m_χ within the Galactic halo, the gamma-ray flux observed at Earth along a line of sight at angle ψ from the Galactic center, with an initial photon energy spectrum per annihilation given by dN_γ/dE , reads

$$\frac{d\Phi_\gamma}{dE} = \frac{1}{2} \frac{\langle\sigma v\rangle_{\text{total}}}{4\pi m_\chi^2} \frac{dN_\gamma}{dE} \frac{\mathcal{J}(\psi)}{J_0}, \quad (28)$$

where

$$\mathcal{J}(\psi) = J_0 \int_0^{\ell_{\text{max}}} \rho^2 \left(\sqrt{R_{\text{sc}}^2 - 2\ell R_{\text{sc}} \cos \psi + \ell^2} \right) d\ell, \quad (29)$$

is the integrated DM density squared and $J_0 = 1/[8.5 \text{ kpc} \times (0.3 \text{ GeV cm}^{-3})^2]$ is an arbitrary normalization constant used to make $\mathcal{J}(\psi)$ dimensionless.

This form of the expression is useful as it factorizes \mathcal{J} , which depends on astrophysics, from the rest of the expression which depends on particles physics. With knowledge of \mathcal{J} for the studied annihilation region and the gamma-ray spectrum per annihilation dN_γ/dE , a constraint can be placed on the thermally averaged self-annihilation cross-section, $\langle\sigma v\rangle_{\text{total}}$. A constraint on this parameter depends only on the spectrum of SM particles per annihilation, not on the underlying particle physics model. The numerical tool introduced in Ref. [133] is helpful to get the spectrum of SM particles in the final state of DM annihilations. Since this spectrum is unknown, searches typically present constraints on individual channels assuming 100% branching ratio to that channel. For example, a search may present a constraint assuming annihilation purely to W^+W^- . This is equivalent to a constraint on the total cross section scaled by the branching ratio to that final state, $\langle\sigma v\rangle_{W^+W^-} \equiv \langle\sigma v\rangle_{\text{total}} \times BR(W^+W^-)$.

This means that an EFT analysis is not strictly necessary for indirect detection studies, since the calculation of the branching ratios within a specific model only adds model-dependence to the constraints.

There are specific cases where EFT can be useful, such as if one is interested in the spectrum of gamma-rays from DM annihilation taking into account all final states. For example, Ref. [134] used effective operators to study whether DM can produce the spectrum of a potential gamma-ray excess from the galactic center, and Refs. [12, 135–138] uses the EFT formalism to calculate the DM annihilation rate to the $\gamma\gamma$ final state. This is a very clean signature with few astrophysical backgrounds, and so determining an accurate branching ratio to this final state can give very strong constraints on DM models.

Effective operators are also useful as a way to compare the strength of indirect detection constraints with constraints from other searches such as direct detection experiments and colliders [13, 18, 29, 139–141].

Galactic WIMPs at the electroweak scale are non-relativistic, and so the energy scale of the interaction is of order $2m_\chi$. Hence the EFT approximation is valid for indirect detection experiments as long as the DM mass is much lighter than the mediator mass.

The operators describing DM interactions with the SM can be organized in the non-relativistic limit as an expansion in their mass dimension and in their velocity dependence (e.g. *s*-wave, *p*-wave, etc. annihilations). For self-conjugate DM (a Majorana fermion or a real scalar field), DM annihilation to light fermions suffers from helicity suppression which can be lifted by including extra gauge boson radiation. This effect is of particular relevance for indirect detection, as it can significantly change the energy spectra of stable particles originating from DM annihilations [18, 142–155]. Sticking to the EFT framework, this effect is encoded by higher-dimensional operators [44, 141].

Indirect detection can also be used to constrain the WIMP-nucleon scattering rate via neutrinos from the sun. As the solar system passes through the Galactic DM halo, DM will scatter with the sun and become gravitationally bound. The DM annihilation rate depends on the square of the DM number density, and therefore after a sufficient amount of time has passed, the DM annihilation rate will increase until it reaches equilibrium with the scattering rate. Therefore the size of the scattering rate will control the flux of particles from the sun from DM annihilation. Due to the opacity of the sun, neutrinos are the only observable DM annihilation product from the sun, and so IceCube and other neutrino observatories can use limits on the neutrino flux from the sun to place constraints on the DM scattering cross-section [156]. This means that indirect detection is in the unique position of being able to probe both the relativistic and non-relativistic DM-SM effective operators.

3 A paradigm shift: Simplified Models

In the previous section we have spelled out the virtues and drawbacks of the EFT approach for DM searches. The significant limitations to a consistent use of effective operators in the context of collider searches justify a paradigm shift beyond the effective-operator approximation.

As anticipated in the Introduction to this review, a possible alternative approach consists of expanding the contact interaction of DM with the SM and include the “mediator” as propagating degrees of freedom of the theory. By increasing the number of parameters necessary to specify the unknown DM interactions one gains a more complete theoretical control.

In this section we will summarize the phenomenology of the simplified models for DM and, wherever available, provide the most important results concerning the collider searches, the DM self-annihilation cross sections and the cross sections for DM scattering with nucleons.

So far, as is customary when discussing EFTs, we have followed a bottom-up approach: the list of effective operators comes purely from symmetry and dimensional analyses. The shift to simplified models now makes it more advantageous to reverse the logic and use a top-down approach from here on. We will categorize the models according to the quantum numbers of the DM particle and the mediator, and to the mediator type (s- or t-channel); see Table 9. This classification refers to $2 \rightarrow 2$ tree-level processes and the model names we choose are designed as an easy-to-recall nomenclature.

We have decided to limit the discussion to scalar and fermion DM only, and not to include in the list the cases where the DM is a massive vector particle. In the spirit of the simplified models, the smallest possible number of degrees of freedom should be added to the SM. Also, the model building with vector DM is necessarily more involved. Furthermore, DM searches at the LHC are based on counting analyses, for which the DM spin is typically not very relevant. Event topologies more complex than the $\cancel{E}_T + j$ can be constructed, along with angular variables [62, 92], which would also allow the exploration of

Mediator spin	Channel	DM spin	Model Name	Discussed in Section
0	s	0	$0s0$	3.2.1
0		$\frac{1}{2}$	$0s\frac{1}{2}$	3.2.2
0		0	$0t0$	3.2.3
0		$\frac{1}{2}$	$0t\frac{1}{2}$	3.2.4
$\frac{1}{2}$	t	0	$\frac{1}{2}t0$	3.3.1
$\frac{1}{2}$		$\frac{1}{2}$	$\frac{1}{2}t\frac{1}{2}$	3.3.2
1	s	0	$1s0$	3.4.1
1		$\frac{1}{2}$	$1s\frac{1}{2}$	3.4.2
1		$\frac{1}{2}$	$1t\frac{1}{2}$	3.4.3

Table 9: Simplified models for scalar and fermion DM.

the spin of the DM particle, to some extent. However, we believe that at the present stage of LHC searches for DM, the simplified models discussed in this review already capture a very rich phenomenology.

Before reviewing the features and the phenomenology of all the cases listed in Table 9, we first point out some general properties of simplified models.

3.1 General properties of simplified models

As discussed above, when building a simplified model for DM one wants to extend the SM by adding new degrees of freedom: not too many, otherwise simplicity is lost; not too few, otherwise the relevant physics is not described completely. To this end, one builds simplified models according to the following general prescriptions:

- (i) the SM is extended by the addition of a DM particle, which is absolutely stable (or, at least, stable on collider scale).
- (ii) The new Lagrangian operators of the models are renormalizable and consistent with the symmetries: Lorentz invariance, SM gauge invariance, DM stability.

In addition to these exact symmetries, the SM has other important global symmetries. Baryon and lepton number are anomalous, but they can be treated as exact symmetries at the renormalizable level. So, we require that simplified models respect baryon and lepton number.

On the other hand, the flavor symmetry of the SM can be broken by new physics, but we need to ensure this breaking is sufficiently small to agree with high-precision flavor experiments. One very convenient approach to deal with this is to impose that new physics either respect the SM flavor symmetry or the breaking of it is associated with the quark Yukawa matrices.

This idea is known as Minimal Flavor Violation (MFV) [157]. It also allows us to keep small the amount of CP violating effects which are possibly induced by new physics. Throughout this paper we will adopt MFV, although it would be interesting to have results for simplified models also in the very constrained situations where this assumption is relaxed.

Following the guidelines outlined above, we now proceed to build and discuss the phenomenology of simplified models.

3.2 Scalar Mediator

The simplest type of simplified model is the one where a scalar particle mediates the interaction between DM and the SM. Their interaction can occur via s-channel or t- channel diagrams. The scalar mediator could be real or complex. In the complex case, it has both scalar and pseudoscalar components. We will separately discuss the cases where the mediator is a purely scalar or a purely pseudoscalar particle.

As for the DM, it may either be a scalar ($0s0$ model) or a Dirac or Majorana fermion ($0s\frac{1}{2}$ model). The more complex possibility of a fermion DM being a mixture of an EW singlet and doublet will be discussed later, as it leads to a hybrid $0s\frac{1}{2}/1s\frac{1}{2}$ model.

The primary focus will be on the tree-level mediator couplings to SM fermions (and the couplings to gluons arising at one loop), being the most important for LHC phenomenology.

An important aspect to keep in mind when dealing with scalar mediators is that they generically mix with the neutral Higgs. In turn, this would affect the Yukawa couplings and the tree-level vertices of the Higgs with two gauge bosons. Such deviations with respect to SM Higgs couplings are severely constrained by Higgs production and decay measurements, although not excluded completely. A common approach in the literature is to simply set the mixing of the scalar mediator with the Higgs to zero, thus keeping the minimal possible set of parameters.

On the other hand one must also consider the possibility that the Higgs boson itself can serve as a scalar mediator between the DM and the rest of the SM, thus providing a rather economical scenario in terms of new degrees of freedom, and sometimes a richer phenomenology. Connecting the DM sector to the SM via the Higgs field may have also interesting consequences for the electroweak symmetry breaking and the Higgs vacuum stability, and it is possible to link the solutions of the hierarchy problem and of the DM problem in a unified framework [158–164].

3.2.1 Scalar DM, s-channel (0s0 model)

In the case where DM is a real scalar singlet ϕ , the mediation is via s-channel and the mediator is a neutral scalar. The most minimal choice is to consider the Higgs boson h as a mediator, rather than a speculative dark sector particle [65, 80, 83, 159, 165–167].

Such a model is described by the Lagrangian

$$\mathcal{L}_{0s0} = \frac{1}{2}(\partial_\mu \phi)^2 - \frac{1}{2}m_\phi^2\phi^2 - \frac{\lambda_\phi}{2\sqrt{2}}vh\phi^2 \quad (30)$$

with $v = 246$ GeV. The DM coupling term of the form ϕ^4 does not play a relevant role for LHC phenomenology and it will be neglected.

The low-energy Lagrangian (30) needs to be completed, at energies larger than m_h , in a gauge-invariant way, using the Higgs doublet H

$$\mathcal{L}_{0s0} = \frac{1}{2}(\partial_\mu \phi)^2 - \frac{1}{2}m_\phi^2\phi^2 - \frac{\lambda_\phi}{4}\phi^2 H^\dagger H \quad (31)$$

Note that this model is described by renormalizable interactions. A discrete Z_2 symmetry under which H is even and ϕ is odd would make ϕ stable and prevent $\phi - H$ mixing.

The model parameters are simply $\{m_\phi, \lambda_\phi\}$ and one can distinguish two main regimes: $m_\phi < m_h/2$, $m_\phi > m_h/2$.

Collider

For DM lighter than half of the Higgs mass ($m_\phi < m_h/2$), the Higgs can decay on-shell to a DM pair. The main collider constraint comes from the invisible width of the Higgs, say $\Gamma_{h,inv}/\Gamma_h \lesssim 20\%$. The Higgs to DM decay responsible for the invisible width is

$$\Gamma(h \rightarrow \phi\phi) = \frac{\lambda_\phi^2}{32\pi} \frac{v^2}{m_h} \sqrt{1 - \frac{4m_\phi^2}{m_h^2}}. \quad (32)$$

Taking $\Gamma_h = 4.2$ MeV for $m_h = 125.6$ GeV, the 20% constraint gives $\lambda_\phi \lesssim 10^{-2}$.

In the opposite regime ($m_\phi > m_h/2$), the invisible width constraint does not apply anymore. The cross-section for DM production at the LHC is further suppressed by λ_ϕ^2 and phase space, thus making mono-jet search strategies irrelevant. The most important constraint for this region of parameter space is on the spin-independent (SI) scattering cross-section from direct detection experiments.

DM self-annihilation

Using (30), the DM self-annihilation cross section to SM fermions of mass m_f is

$$\langle\sigma v_{\text{rel}}\rangle(\phi\phi \rightarrow \bar{f}f) = \frac{\lambda_\phi^2 m_f^2}{8\pi} \frac{\left(1 - \frac{m_f^2}{m_\phi^2}\right)^{3/2}}{(m_h^2 - 4m_\phi^2)^2 + m_h^2\Gamma_h^2} + \mathcal{O}(v_{\text{rel}}^2) \quad (33)$$

where v_{rel} is the relative velocity of DM particles.

Using the high-energy completion Eq. (31), the annihilation to hh final states also opens up,

$$\langle\sigma v_{\text{rel}}\rangle(\phi\phi \rightarrow hh) = \frac{\lambda_\phi^2}{512\pi m_\phi^2}, \quad (m_h = 0). \quad (34)$$

DM scattering on nucleons

The effective Lagrangian at the DM-quark level is

$$\mathcal{L}_{\text{eff}} = \sum_q \frac{y_q \lambda_\phi v}{4m_h^2} \phi^2 \bar{q}q \quad (35)$$

where the Yukawa coupling y_q is defined by $m_q = y_q v / \sqrt{2}$. The DM-nucleon scattering cross section is given by Eq. (20), with coefficient (cf. Table 8)

$$\begin{aligned} c^N &= \sum_{q=u,d,s} \frac{y_q \lambda_\phi v}{4m_h^2} \frac{m_N}{m_q} f_q^{(N)} + \frac{2}{27} f_G^{(N)} \left(\sum_{q=c,b,t} \frac{y_q \lambda_\phi v}{4m_h^2} \frac{m_N}{m_q} \right) \\ &= \frac{\lambda_\phi m_N}{2\sqrt{2}m_h^2} \left(\sum_{q=u,d,s} f_q^{(N)} + \frac{6}{27} \left(1 - \sum_{q=u,d,s} f_q^{(N)} \right) \right), \end{aligned} \quad (36)$$

where $f_q^{(N)}$ are given in Table 7, and recalling that $f_G^{(N)} \equiv 1 - \sum_{q=u,d,s} f_q^{(N)}$

3.2.2 Fermion DM, *s*-channel ($0s\frac{1}{2}$ model)

■ GENERIC CASE

The next case we would like to consider is a spin-1/2 DM particle, taken to be a Dirac fermion. The Majorana case only involves some minor straightforward changes.

We consider two benchmark models where the gauge-singlet mediator is either a scalar S or a pseudoscalar A , described by the Lagrangians

$$\mathcal{L}_{0s\frac{1}{2}} = \frac{1}{2} (\partial_\mu S)^2 - \frac{1}{2} m_S^2 S^2 + \bar{\chi} (i\cancel{d} - m_\chi) \chi - g_\chi S \bar{\chi} \chi - g_{\text{SM}} S \sum_f \frac{y_f}{\sqrt{2}} \bar{f} f, \quad (37)$$

$$\mathcal{L}_{0A\frac{1}{2}} = \frac{1}{2} (\partial_\mu A)^2 - \frac{1}{2} m_A^2 A^2 + \bar{\chi} (i\cancel{d} - m_\chi) \chi - i g_\chi A \bar{\chi} \gamma^5 \chi - i g_{\text{SM}} A \sum_f \frac{y_f}{\sqrt{2}} \bar{f} \gamma^5 f, \quad (38)$$

where the sum runs over SM fermions f . The DM particle is unlikely to receive its mass from electroweak symmetry breaking, so its interaction with the mediator has not been set proportional to a Yukawa coupling.

As for the operators connecting the mediators to SM fermions, the MFV hypothesis requires the coupling to be proportional to the Yukawas y_f . However, in full generality it is possible to have non-universal g_{SM} couplings, e.g. $g_{\text{SM}}^{(u)} \neq g_{\text{SM}}^{(d)} \neq g_{\text{SM}}^{(\ell)}$, for up-type quarks, down-type quarks and leptons. Notably, the situation where $g_{\text{SM}}^{(u)} \neq g_{\text{SM}}^{(d)}$ arises in Two-Higgs-Doublet Models. In the following we will focus on the universal couplings, but the reader should keep in mind that this is not the most general situation.

Another caveat concerns the mixing of the scalar mediator with the Higgs. In general, Lagrangian operators mixing a gauge singlet scalar with a Higgs doublet (e.g. $S^2 |H|^2$) are allowed. As discussed in the introduction of Section 3.2 we will follow the common assumption by neglecting these mixings. However, we will later discuss an example of these when discussing the Two-Higgs-Doublet Model (2HDM).

So, the simplified models described by equations (37) and (38) have a minimal parameter count:

$$\{m_\chi, m_{S/A}, g_\chi, g_{\text{SM}}\}. \quad (39)$$

Collider

The mediators have decay channels to SM fermions, DM particles or to gluons (via a fermion loop dominated by the top-quark). The corresponding partial widths are

$$\Gamma(S/A \rightarrow \bar{f}f) = \sum_f N_c(f) \frac{y_f^2 g_{\text{SM}}^2 m_{S/A}}{16\pi} \left(1 - \frac{4m_f^2}{m_{S/A}^2}\right)^{n/2} \quad (40)$$

$$\Gamma(S/A \rightarrow \bar{\chi}\chi) = \frac{g_\chi^2 m_{S/A}}{8\pi} \left(1 - \frac{4m_\chi^2}{m_{S/A}^2}\right)^{n/2} \quad (41)$$

$$\Gamma(S/A \rightarrow gg) = \frac{\alpha_s^2 y_t^2 g_{\text{SM}}^2}{32\pi^3} \frac{m_{S/A}^3}{v^2} \left| f_{S/A} \left(\frac{4m_t^2}{m_{S/A}^2} \right) \right|^2 \quad (42)$$

where $N_c(f)$ is the number of colors of fermion f (3 for quarks, 1 for leptons), and $n = 1$ for pseudoscalars, 3 for scalars. The loop functions are

$$f_S(\tau) = \tau \left[1 + (1 - \tau) \arctan^2 \frac{1}{\sqrt{\tau - 1}} \right] \quad (43)$$

$$f_A(\tau) = \tau \arctan^2 \frac{1}{\sqrt{\tau - 1}} \quad (44)$$

for $\tau > 1$.

Other loop-induced decay channels, such as decay to $\gamma\gamma$, are sub-dominant. Of course, in the presence of additional (possibly invisible) decay modes of the mediators, the total width will be larger than the sum of the partial widths written above.

Typically, the decay to DM particles dominates, unless the mediator is heavy enough to kinematically open the decay to top-quarks. Also notice the different scaling with respect to DM velocity $(1 - 4m_f^2/m_{S/A}^2)^{n/2}$ for scalars and pseudoscalars. In the region close to the kinematic boundary, the decay width of A is larger and therefore one expects stronger constraints on pseudoscalars than on scalars.

There are three main strategies to search for this kind of simplified model at colliders: MET with 1 jet ($\cancel{E}_T + j$), MET with 2 top-quarks ($\cancel{E}_T + t\bar{t}$), MET with 2 bottom-quarks ($\cancel{E}_T + b\bar{b}$), see Fig. 2.

The $\cancel{E}_T + j$ searches are expected to provide the strongest discovery potential, but the channels with heavy quarks tagged can have much lower backgrounds, and they can get more and more relevant as the energy and the luminosity of LHC is increasing.

DM self-annihilation

The self-annihilations of two DM particles are the key processes to consider when studying the relic abundance (freeze-out mechanism in the early universe) or the indirect detection constraints (constraints from observations of DM annihilation products, usually studying annihilation in the halo or galactic center today).

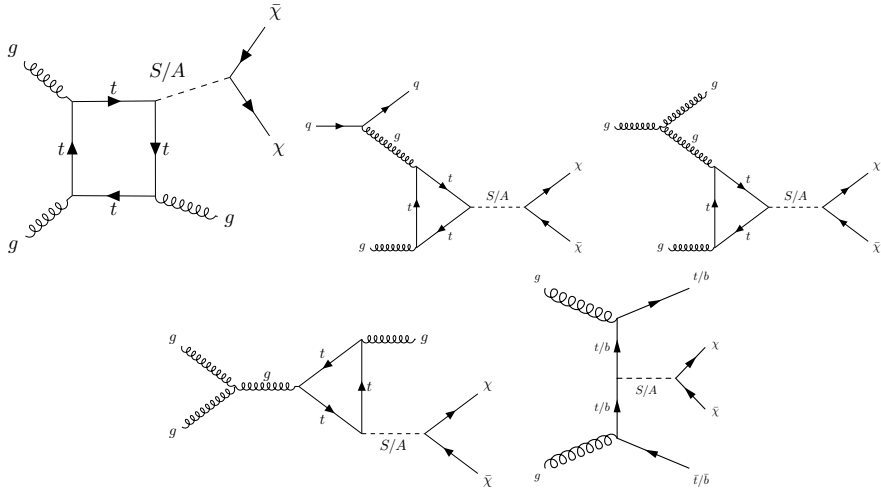


Fig. 2: Diagrams contributing to $\cancel{E}_T + j$, $\cancel{E}_T + t\bar{t}$ and $\cancel{E}_T + b\bar{b}$ signals. The $\cancel{E}_T + j$ diagrams involve loop of top-quarks, while $\cancel{E}_T + t\bar{t}$, $\cancel{E}_T + b\bar{b}$ involve tree-level emission of mediator from a t -channel top-quark exchange. Most Feynman diagrams were generated using TikZ-Feynman [168].

The thermally averaged self-annihilation cross sections of Dirac DM χ , via a scalar or pseudoscalar mediator, to SM fermions f are

$$\langle\sigma v_{\text{rel}}\rangle(\phi\phi \rightarrow S \rightarrow \bar{f}f) = N_c(f) \frac{g_\chi^2 g_{\text{SM}}^2 y_f^2}{16\pi} \frac{m_\chi^2 \left(1 - \frac{m_f^2}{m_\chi^2}\right)^{3/2}}{(m_S^2 - 4m_\chi^2)^2 + m_S^2 \Gamma_S^2} v_{\text{rel}}^2 \quad (45)$$

$$\langle\sigma v_{\text{rel}}\rangle(\phi\phi \rightarrow A \rightarrow \bar{f}f) = N_c(f) \frac{g_\chi^2 g_{\text{SM}}^2 y_f^2}{4\pi} \frac{m_\chi^2 \left(1 - \frac{m_f^2}{m_\chi^2}\right)^{1/2}}{(m_A^2 - 4m_\chi^2)^2 + m_A^2 \Gamma_A^2}. \quad (46)$$

For Majorana DM, the above cross-sections get multiplied by 2. Notice that the annihilation via scalar mediator is in p -wave (v^2 -suppressed) even for $m_f \neq 0$.

DM scattering on nucleons

In the low-energy regime at which DM-nucleon scattering is taking place, it is possible to integrate out the mediator and recover the EFT description, with the operators

$$\mathcal{O}_S = \frac{g_\chi g_{\text{SM}} y_q}{\sqrt{2} m_S^2} (\bar{\chi} \chi) (\bar{q} q) = \frac{g_\chi g_{\text{SM}} y_q}{\sqrt{2} m_S^2} \mathcal{O}_{D1} \quad (47)$$

$$\mathcal{O}_A = \frac{g_\chi g_{\text{SM}} y_q}{\sqrt{2} m_A^2} (\bar{\chi} i\gamma^5 \chi) (\bar{q} i\gamma^5 q) = \frac{g_\chi g_{\text{SM}} y_q}{\sqrt{2} m_A^2} \mathcal{O}_{D4} \quad (48)$$

describing the DM-quarks fundamental scattering, and expressed in terms of the operators in Table 1. Remember that the operator coefficients must be evaluated at the scale where

scattering is occurring [89, 122], by performing RG evolution from the high energy theory as well as matching conditions at the quark mass thresholds.

The scalar exchange gives rise to spin-independent DM-nucleon scattering, while the pseudoscalar gives a spin and momentum suppressed cross-section. The latter case does not provide significant constraints from direct detection experiments. As for the SI case, the elastic DM-nucleon cross section (for Dirac DM) is given by Eq. (20), with effective coupling (cf. Table 6)

$$\begin{aligned} c^N &= \sum_{q=u,d,s} f_q^{(N)} \frac{m_N}{m_q} \left(\frac{g_\chi g_{\text{SM}} y_q}{\sqrt{2} m_S^2} \right) + \frac{2}{27} f_G^{(N)} \sum_{q=c,b,t} \frac{m_N}{m_q} \left(\frac{g_\chi g_{\text{SM}} y_q}{\sqrt{2} m_S^2} \right) \\ &= \left(\frac{g_\chi g_{\text{SM}}}{v m_S^2} \right) m_N \left[\sum_{q=u,d,s} f_q^{(N)} + \frac{6}{27} \left(1 - \sum_{q=u,d,s} f_q^{(N)} \right) \right]. \end{aligned} \quad (49)$$

where we have again used that $f_G^{(N)} = 1 - \sum_{q=u,d,s} f_q^{(N)}$ and that g_{SM} was assumed to be flavor-universal, otherwise one cannot take that factor out of the sum over quarks. Sample numerical values of the couplings $f_q^{(N)}$ are listed in Table 7.

■ CASE STUDY 1: HIGGS AS MEDIATOR

As a first case study, we consider one specific realisation of the $0s\frac{1}{2}$ model outlined earlier, where the Higgs itself serves as the scalar mediator particle. We already considered this possibility in Section 3.2.1 for the case of scalar DM ($0s0$ model). Here we want to outline the main features of this ‘‘Higgs portal’’ model for Dirac fermion DM [82, 86, 169, 170].

The Lagrangian of the model at low energies is

$$\mathcal{L} \supset -\frac{h}{\sqrt{2}} \left[\sum_f y_f \bar{f} f + \bar{\chi} (y_\chi + i y_\chi^P \gamma^5) \chi \right] \quad (50)$$

which can be matched to the Lagrangians Eqs. (37) and (38) of Section 3.2.2, provided that $y_\chi = g_\chi \sqrt{2}$, or $y_\chi^P = g_\chi \sqrt{2}$, $g_{\text{SM}} = 1$.

Notice, however, that here the Higgs h is a real scalar field (not a pseudoscalar, like the generic mediator A); so the pseudoscalar coupling in Eq. (50) only affects the h -DM interaction and not the usual Yukawa interactions between the Higgs and the SM fermions f . So the generic pseudoscalar model $0_A s\frac{1}{2}$ cannot be completely matched with the model in Eq. (50) since the Higgs is a real scalar.

At energies larger than the Higgs mass, the effective Lagrangian in Eq. (50) is completed in a gauge-invariant way as

$$\mathcal{L} \supset -\frac{H^\dagger H}{2v} \bar{\chi} (y_\chi + i y_\chi^P \gamma^5) \chi \quad (51)$$

which is described by a dimension-5 operator.

The model parameters are simply $\{m_\chi, y_\chi\}$ or $\{m_\chi, y_\chi^P\}$, if one considers the scalar and pseudoscalar couplings separately.

Collider

For DM lighter than half of the Higgs mass ($m_\chi < m_h/2$), the on-shell decays of the Higgs into a DM pair contribute to the Higgs invisible width

$$\Gamma(h \rightarrow \bar{\chi}\chi) = \frac{y_\chi^2 m_h}{16\pi} \left(1 - \frac{4m_\chi^2}{m_h^2}\right)^{3/2} \quad (52)$$

or

$$\Gamma(h \rightarrow \bar{\chi}\chi) = \frac{(y_\chi^P)^2 m_h}{16\pi} \left(1 - \frac{4m_\chi^2}{m_h^2}\right)^{1/2} \quad (53)$$

The experimental constraint $\Gamma_{h,inv}/\Gamma_h \lesssim 20\%$ gives $y_\chi, y_\chi^P \lesssim 10^{-2}$, for $\Gamma_h = 4.2$ MeV and $m_h = 125.6$ GeV [114].

The opposite mass regime $m_\chi > m_h/2$ is not significantly constrained by collider data, for couplings within the perturbative domain.

DM self-annihilation

The thermally-averaged annihilation cross sections for Dirac fermion DM are

$$\langle\sigma v_{\text{rel}}\rangle(\chi\chi \rightarrow \bar{f}f) = N_c(f) \frac{y_\chi^2 y_f^2}{32\pi} \frac{m_\chi^2 \left(1 - \frac{m_f^2}{m_\chi^2}\right)^{3/2}}{(m_h^2 - 4m_\chi^2)^2 + m_h^2 \Gamma_h^2} v_{\text{rel}}^2 \quad (54)$$

$$\langle\sigma v_{\text{rel}}\rangle(\chi\chi \rightarrow \bar{f}f) = N_c(f) \frac{(y_\chi^P)^2 y_f^2}{8\pi} \frac{m_\chi^2 \left(1 - \frac{m_f^2}{m_\chi^2}\right)^{3/2}}{(m_h^2 - 4m_\chi^2)^2 + m_h^2 \Gamma_h^2}. \quad (55)$$

For Majorana DM one needs to include an extra factor of 2.

The scalar coupling does not produce s -wave cross sections. For DM masses above the Higgs mass, the Lagrangian operator Eq. (51) opens up self-annihilations to two Higgses or longitudinal gauge bosons

$$\langle\sigma v_{\text{rel}}\rangle(\chi\chi \rightarrow HH) = \frac{1}{64\pi v^2} \left[(y_\chi^P)^2 + \frac{v_{\text{rel}}^2}{4} y_\chi^2 \right]. \quad (56)$$

DM scattering on nucleons

At low energies, after integrating out the Higgs field, we end up with the effective Lagrangian

$$\mathcal{L}_{\text{eff}} \supset \frac{y_f}{2m_h^2} (\bar{q}q) \left[\bar{\chi}(y_\chi + i\gamma^5 y_\chi^P)\chi \right]. \quad (57)$$

The coupling y_χ multiplies the \mathcal{O}_{D1} operator while y_χ^P is in front of a \mathcal{O}_{D2} operator. Therefore, the scalar coupling is responsible for spin-independent cross section, while the pseudoscalar coupling drives a spin and momentum dependent cross-section, as described in section 2.2. The spin-independent cross section can be found via Eqn. (20) with coefficient

$$c^N = \frac{y_\chi m_N}{\sqrt{2} v m_h^2} \left[\sum_{q=u,d,s} f_q^{(N)} + \frac{6}{27} \left(1 - \sum_{q=u,d,s} f_q^{(N)}\right) \right] \quad (58)$$

The current best limits on spin-independent cross-section from LUX [171] rule out a fermion DM coupling to Higgs with the correct thermal relic abundance for $m_\chi \lesssim 10^3$ GeV. However,

unknown particles/interactions may reduce the abundance of DM coupled to Higgs and relax the tension with DD data.

On the other hand, because of much weaker constraints on spin and momentum suppressed cross sections, there are currently no limits on perturbative values of y_χ^P from direct detection, thus leaving this case as still viable.

■ CASE STUDY 2: TWO-HIGGS-DOUBLET MODEL (2HDM)

Another specific realization of the $0s\frac{1}{2}$ model arises by allowing mixing between a real scalar mediator S and the Higgs boson. In this case, to keep the model as minimal as possible, the mediator S is not allowed to have couplings directly to the SM fermions, but only through the “Higgs portal”. Therefore, this kind of model looks like a 2HDM extension of the SM Higgs sector. The DM is again assumed to be a Dirac fermion and the Lagrangian describing the model is

$$\begin{aligned} \mathcal{L} \supset & \frac{1}{2}(\partial_\mu S)^2 - \frac{1}{2}m_S^2 S^2 + \bar{\chi}(i\cancel{d} - m_\chi)\chi - \frac{h}{\sqrt{2}} \sum_f y_f \bar{f}f \\ & - y_\chi S \bar{\chi}\chi - \mu_S S |H|^2 - \lambda_S S^2 |H|^2. \end{aligned} \quad (59)$$

The cubic and quartic self-couplings of the mediator S do not play any role for LHC phenomenology and they have not been considered in the Lagrangian. Another simplification is to forbid the S mediator from developing a VEV, $\langle S \rangle = 0$. The generalization where this assumption is relaxed is straightforward.

This model is described by the 4 parameters: $\{m_\chi, m_S, \lambda_S, \mu_S\}$. The mediator-Higgs mixing driven by μ_S leads us to diagonalize the mass matrix and find the physical mass eigenstates h_1 and h_2

$$\begin{pmatrix} h_1 \\ h_2 \end{pmatrix} = \begin{pmatrix} \cos \theta & \sin \theta \\ -\sin \theta & \cos \theta \end{pmatrix} \begin{pmatrix} h \\ S \end{pmatrix}, \quad (60)$$

where the mixing angle is defined by $\tan(2\theta) = 2\mu_S/(m_S^2 - m_h^2 + \lambda_S v^2)$, in such a way that $\theta = 0$ ($\mu_S = 0$) corresponds to a dark sector decoupled from the SM, and the physical masses are approximately given by

$$m_{h_1} \simeq m_h \quad (61)$$

$$m_{h_2} \simeq \sqrt{m_S^2 + \lambda_S^2 v^2}, \quad (62)$$

so that h_1 corresponds to the physical Higgs boson of mass ~ 125 GeV.

In the mass-eigenstate basis, the Lagrangian (59) reads

$$\mathcal{L} \supset -(h_1 \cos \theta - h_2 \sin \theta) \sum_f \frac{y_f}{\sqrt{2}} \bar{f}f - (h_1 \sin \theta + h_2 \cos \theta) y_\chi \bar{\chi}\chi. \quad (63)$$

This Lagrangian is of the same form as the generic one $\mathcal{L}_{0s\frac{1}{2}}$ of Eq. (37), where we can identify h_2 with S and read the corresponding couplings

$$g_\chi = y_\chi \cos \theta \quad (64)$$

$$g_{\text{SM}} = -\sin \theta, \quad (65)$$

while the Higgs Yukawa couplings to fermions are reduced as $y_f \cos \theta$.

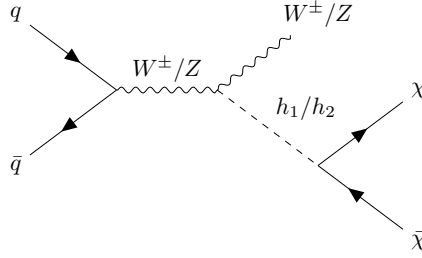


Fig. 3: Diagram of the process contributing to mono-W/Z signals in 2HDM.

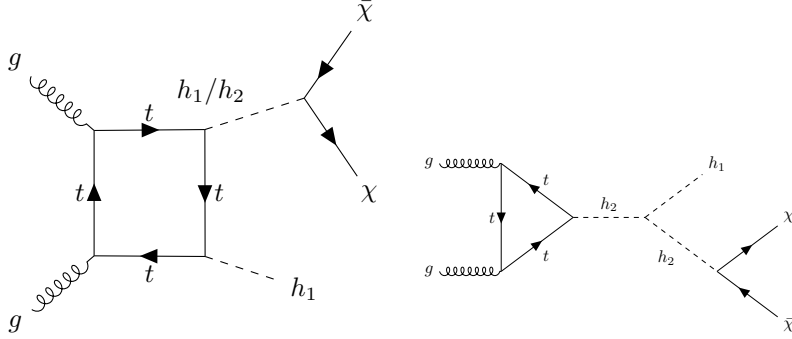


Fig. 4: Diagrams contributing to mono-Higgs signals in 2HDM.

Collider

In addition to the Yukawa couplings, the $\cos \theta$ suppression also appears in the trilinear couplings of the Higgs with two gauge bosons, and therefore θ is constrained by Higgs physics measurements as well as EW precision tests. The limits from LHC Run I Higgs physics are the most stringent ones and give $\sin \theta \lesssim 0.4$ [172, 173].

The invisible width of the Higgs decaying to DM particles is

$$\Gamma(h_1 \rightarrow \chi\bar{\chi}) \frac{y_\chi^2 \sin^2 \theta m_{h_1}}{8\pi} \left(1 - \frac{4m_\chi^2}{m_{h_1}^2}\right)^{3/2}, \quad (66)$$

and for a light enough mediator, the $h_1 \rightarrow h_2 h_2$ decay can also open up. The calculation of the invisible BR of the Higgs should also take into account that the Higgs decays to SM fermions receive a $\cos^2 \theta$ suppression.

On top of the usual $\cancel{E}_T + j$ signal, the 2HDM-like simplified model possesses other interesting channels that may distinguish it from the generic scalar mediator case. For instance, mono-W/Z signals can arise at tree level as in Fig. 3.

An important feature is the destructive interference between the exchange of h_1 and h_2 , which has an impact on both LHC and DD phenomenology.

Furthermore, the $h_1 h_2^2$ trilinear vertex is likely to change the phenomenology of mono-Higgs signals by adding to the usual diagram (Fig. 4 left), and the diagram with triangle top-loop (Fig. 4 right).

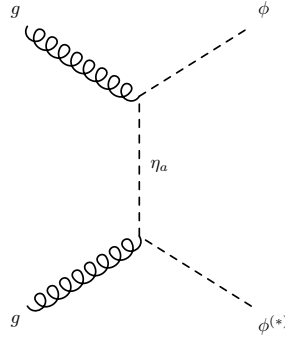


Fig. 5: Diagram for DM pair production in 0t0 model.

DM self-annihilation and scattering on nucleons

The DM self-annihilation rate and scattering rate are identical to the generic case with scalar mediator described by Eqs. (45), (49) respectively, with the couplings g_χ, g_{SM} replaced with the expressions in Eqs. (64), (65).

3.2.3 Scalar DM, t -channel (0t0 model)

So far we have discussed models where the mediator particle is exchanged in the s -channel, but it is also possible to build simplified models where the mediator exchange is via the t -channel.

The scalar DM particle ϕ cannot be colored, therefore the mediator needs to carry color. Tree-level processes initiated by quarks are not possible because of Lorentz symmetry, therefore the only possibility is to have diagrams with two gluons in the initial state (see Fig. 5). This implies that the scalar mediator η^a is a color octet, $a = 1, \dots, 8$.

A pair of scalar octets can couple at the renormalizable level with one or two gluons, while a single scalar octet can couple to two quarks via a dimension-5 operator proportional to the quark mass, as a consequence of gauge-invariance [174, 175].

At renormalizable level, it is impossible to couple the color-octet mediator η^a with DM and a gluon, therefore such an interaction is suppressed. A color octet can be either singly- or doubly-produced at the LHC via QCD interactions and subsequently decay to two jets. The analysis of the di-jet invariant mass with 4.8 fb^{-1} of data at $\sqrt{s} = 7 \text{ TeV}$ places a bound on m_η to be above 2 TeV at 95% CL [176].

This strong bound, together with the suppressed interaction of the octet with DM, makes it difficult to explore this model in detail at the LHC and in other experiments. Nonetheless, a thorough exploration of this simplified model and its phenomenology is still missing.

3.2.4 Fermion DM, t -channel (0t $\frac{1}{2}$ model)

Let us now turn to consider the most common situation of this kind, where the DM is a spin- $\frac{1}{2}$ (Dirac or Majorana) fermion χ and the mediator is a scalar particle η . The interaction of interest is the one connecting χ and η to a quark field q : $\eta \bar{\chi} q + \text{h.c.}$. Since DM cannot have color charge, η has to be colored. As for flavor, in order to comply with MFV, either η or χ should carry a flavor index. Although models with flavored DM has been considered

[23, 177, 178], we consider here the situation of unflavored DM where η carries flavor index [39, 53–56, 56, 105, 115, 149, 179–181]. In this case the mediator closely resembles the squarks of the MSSM, for which extensive searches already exist (see e.g. [113]).

Having decided that η carries both color and flavor indices, it remains to be seen whether it couples to right-handed quark singlets (up-type or down-type) or to left-handed quark doublets. The choice made here is to couple η to right-handed up-type quarks $u_i = \{u_R, c_R, t_R\}$, so that the Lagrangian for the 3 mediator species η_i reads

$$\mathcal{L}_{0t\frac{1}{2}} \supset \sum_{i=1,2,3} \left[\frac{1}{2} (\partial_\mu \eta_i)^2 - \frac{1}{2} M_i^2 \eta_i^2 + (g_i \eta_i^* \bar{\chi} u_i + \text{h.c.}) \right]. \quad (67)$$

Other choices for mediator-quark interactions can be worked out similarly.

The MFV hypothesis imposes universal masses and couplings $M_1 = M_2 = M_3 \equiv M$ and $g_1 = g_2 = g_3 \equiv g$, thus resulting in a three-dimensional parameter space

$$\{m_\chi, M, g\}. \quad (68)$$

However, the breaking of this universality is possible, resulting in a splitting of the third-generation mediator ($i = 3$) from the first two ($i = 1, 2$).

Stability of DM against decays is ensured by considering $m_\chi < m_\eta$, so that DM decays are not kinematically open.

Collider

Given the similarity of the mediator to squarks, collider searches for this class of model can fruitfully combine usual mono-jet with strategies for squark detection. The main contributions to the $\cancel{E}_T + j$ process come from the diagrams in Fig. 6, relative to the processes $u\bar{u} \rightarrow \bar{\chi}\chi + g$, $u\bar{u} \rightarrow \bar{\chi}\chi + u$, $u\bar{u} \rightarrow \bar{\chi}\chi + \bar{u}$.

Typically, the diagram on the right of Fig. 6 tends to dominate because of larger parton luminosity of the gluon. The gluon radiation from the t -channel mediator is also possible (last diagram of Fig. 6), but it is suppressed by a further $1/M^2$ (it would correspond to a dimension-8 operator in the low-energy EFT).

The mono-jet searches now usually include also a second jet: $\cancel{E}_T + 2j$. These processes are mainly sourced by mediator pair production ($pp \rightarrow \eta_1 \eta_1^*$) followed by mediator splitting ($\eta_1 \rightarrow \chi u$), as in Fig. 7, relative to processes $gg \rightarrow \bar{\chi}\chi \bar{u}u$, $\bar{u}u \rightarrow \bar{\chi}\chi \bar{u}u$. If the DM is a Majorana particle, further mediator pair production processes are possible, initiated by uu or $\bar{u}\bar{u}$ states.

Unlike squark searches, where the squark-neutralino coupling is fixed by supersymmetry to be weak, in the simplified models g_1 is a free parameter. Depending on its magnitude, the relative weights of the diagrams change. For instance, if g_1 is weak ($g_1 \ll g_s$) the QCD pair production dominates over the production through DM exchange.

Comprehensive analyses of collider constraints on t -channel mediator models with fermion DM have been presented in Refs. [54–56, 181]. The combination of mono-jet and squark searches leads to complementary limits. The mono-jet searches are usually stronger in the case where the DM and the mediator are very close in mass.

Before closing this part, it is useful to quote here the result for the mediator width, in the model of Eq. (67)

$$\Gamma(\eta_i \rightarrow \chi \bar{u}_i) = \frac{g_i^2}{16\pi} \frac{M_i^2 - m_\chi^2 - m_{u_i}^2}{M_i^3} \sqrt{(M_i^2 - m_\chi^2 - m_{u_i}^2)^2 - 4m_\chi^2 m_{u_i}^2}. \quad (69)$$

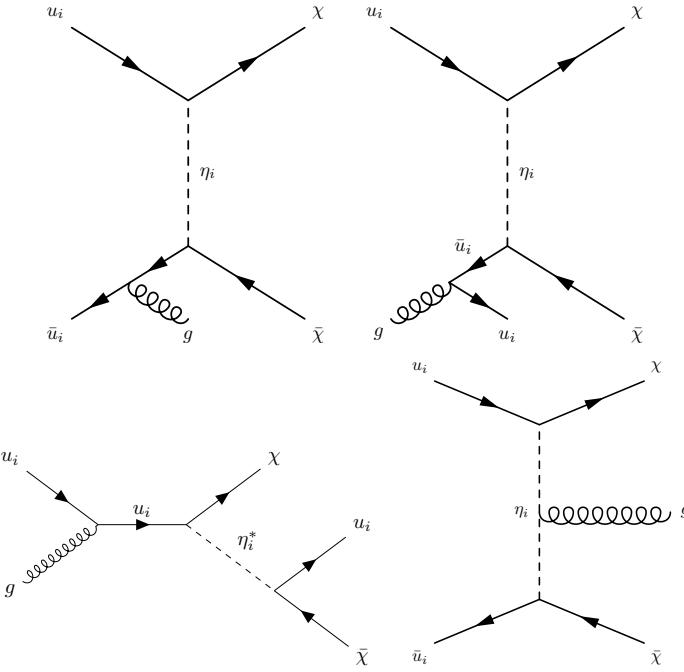


Fig. 6: Diagrams contributing to mono-jet signals in $0t\frac{1}{2}$ model.

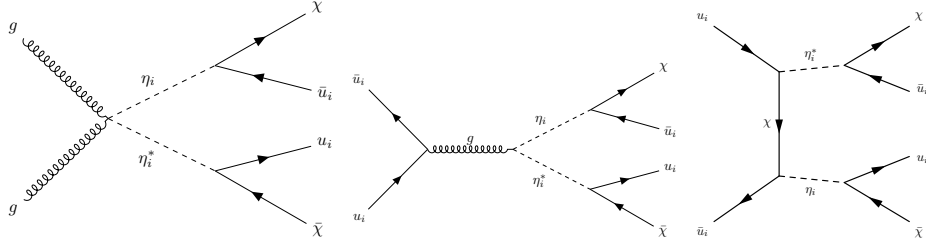


Fig. 7: Diagrams contributing to $\cancel{E}_T + 2j$ signals in $0t\frac{1}{2}$ model.

DM self-annihilation

The main process for DM self-annihilations is $\bar{\chi}\chi \rightarrow \bar{u}_i u_i$, via t -channel exchange of the mediator η_i . This is the relevant process for indirect DM searches.

However, the situation is different for freeze-out calculations. If the DM and the mediator are sufficiently close in mass ($M_i - m_\chi \lesssim T_{\text{freeze-out}}$), coannihilations become relevant and one should also take into account the mediator self-annihilations and the $\chi\eta$ scatterings. The details of these processes are strongly dependent on whether the DM is a Dirac or Majorana fermion.

For Dirac χ ($0t\frac{1}{2}D$ model)

$$\langle\sigma v_{\text{rel}}\rangle(\bar{\chi}\chi \rightarrow \bar{u}_i u_i) = \frac{3g_i^4}{32\pi} \frac{m_\chi^2}{(m_\chi^2 + M_i^2)^2} \quad (m_{u_i} = 0) \quad (70)$$

$$\langle\sigma v_{\text{rel}}\rangle(\chi\eta_i^* \rightarrow u_i g) = \frac{g_s^2 g_i^2}{24\pi} \frac{1}{M_i(m_\chi + M_i)} \quad (m_{u_i} = 0) \quad (71)$$

$$\langle\sigma v_{\text{rel}}\rangle(\eta_i\eta_i^* \rightarrow gg) = \frac{7g_s^4}{216\pi} \frac{1}{M_i^2}, \quad (72)$$

while the process $\eta_i\eta_i^* \rightarrow \bar{u}_i u_i$ is p -wave suppressed.

For Majorana χ ($0t\frac{1}{2}M$ model)

$$\langle\sigma v_{\text{rel}}\rangle(\chi\chi \rightarrow \bar{u}_i u_i) = \frac{g_i^4}{64\pi} \frac{m_\chi^2(m_\chi^4 + M_i^4)}{(m_\chi^2 + M_i^2)^4} v_{\text{rel}}^2 \quad (m_{u_i} = 0) \quad (73)$$

is p -wave suppressed, and

$$\langle\sigma v_{\text{rel}}\rangle(\chi\eta_i^* \rightarrow u_i g) = \frac{g_s^2 g_i^2}{24\pi} \frac{1}{M_i(m_\chi + M_i)} \quad (m_{u_i} = 0) \quad (74)$$

$$\langle\sigma v_{\text{rel}}\rangle(\eta_i\eta_i^* \rightarrow \bar{u}_i u_i) = \frac{g_i^4}{6\pi} \frac{m_\chi^2}{(m_\chi^2 + M_i^2)^2} \quad (m_{u_i} = 0) \quad (75)$$

$$\langle\sigma v_{\text{rel}}\rangle(\eta_i\eta_i^* \rightarrow gg) = \frac{7g_s^4}{216\pi} \frac{1}{M_i^2}. \quad (76)$$

The p -wave suppressed self-annihilation cross section for Majorana DM has been thought to be an issue for studying this model with indirect detection. However, it has been noted that the radiation of an EW gauge boson is able to lift the suppression and open up phenomenologically interesting channels for indirect detection [146–149]. This has interesting implications, as the decay of a radiated massive gauge bosons into hadronic final states means that even if the mediator only couples the DM to leptons, photons and antiprotons will inevitably be produced. Electroweak radiation is in general important to take into account when attempting to explain an observed signal such as the apparent excess in the positron flux [182, 183] without overproducing other standard model particles such as antiprotons [184]. This is especially important in the $0t\frac{1}{2}M$ model when the DM and mediator are near degenerate in mass, as the $2 \rightarrow 3$ process $\bar{\chi}\chi \rightarrow \bar{f}f'V$ can even dominate over the $2 \rightarrow 2$ process $\bar{\chi}\chi \rightarrow \bar{f}f$.

DM scattering on nucleons

As before, the phenomenology is quite different for Dirac and Majorana DM. The DM-nucleon scattering in the low-energy is driven by the effective operator $(\bar{\chi}u_i)(\bar{u}_i\chi)$, which can be expanded using Fierz identities into a sum of s -channel operators in the chiral basis [149]

$$(\bar{\chi}u_i)(\bar{u}_i\chi) = \frac{1}{2}(\bar{\chi}\gamma^\mu P_L\chi)(\bar{u}_i\gamma_\mu P_R u_i) \sim \mathcal{O}_{D5} - \mathcal{O}_{D6} + \mathcal{O}_{D7} - \mathcal{O}_{D8}, \quad (77)$$

where $P_L = \frac{1-\gamma_5}{2}$ and $P_R = \frac{1+\gamma_5}{2}$ are the usual chiral projection operators. If χ is a Dirac fermion, the D5 operator is non-vanishing and provides the spin-independent contribution to the DM-nucleon cross section

$$\sigma_{\chi N}^{\text{SI}} = \frac{g_1^4}{64\pi} \frac{\mu_{\chi N}^2}{(M_1^2 - m_\chi^2)^2} f_N^2 \quad (N = n, p), \quad (78)$$

where $f_n = 1, f_p = 2$ because in the Lagrangian Eq. (67), χ scatters only with up-quarks.

If χ is a Majorana fermion, the D5 and D7 operators vanish identically and the others only contribute to the spin-suppressed scattering operators $\mathcal{O}_4^{\text{NR}}$, $\mathcal{O}_8^{\text{NR}}$ and $\mathcal{O}_9^{\text{NR}}$, listed in Table 5. For Dirac DM ($0t\frac{1}{2}D$), limits from the LHC and direct detection turn out to be incompatible with full relic density abundance from thermal freeze-out. On the other hand, the $0t\frac{1}{2}M$ model with $m_\chi \gtrsim 100$ GeV is still viable. Of course one should keep in mind that bounds from the relic density are not robust, as the DM may not be thermally produced, or thermal production may make only a fraction of the present DM density.

3.3 Fermion Mediator

When the mediator is a fermion, the $2 \rightarrow 2$ scattering process of a pair of colorless DM particles with two SM particles occurs in the t -channel. The DM can either be a scalar ($\frac{1}{2}t0$ model) or a fermion ($\frac{1}{2}t\frac{1}{2}$ model).

3.3.1 Scalar DM, t -channel ($\frac{1}{2}t0$ model)

If the DM is a SM-singlet scalar ϕ , it is possible for the mediator to be a vector-like fermion ψ exchanged in the t -channel. Following Ref. [185], we will consider the Lagrangian

$$\mathcal{L}_{\frac{1}{2}t0} \supset \frac{1}{2}(\partial_\mu \phi)^2 - \frac{1}{2}m_\phi \phi^2 + \bar{\psi}(iD - M_\psi)\psi + (y\phi\bar{\psi}q_R + \text{h.c.}). \quad (79)$$

One can choose to couple the DM and the mediator to any SM right-handed or left-handed fermion. The choice made in Eq. (79) consists of focusing on couplings to right-handed quarks, which plays the major role for LHC and direct detection phenomenology (see Refs. [186, 187] for the lepton case). The discussion for the case of couplings to q_L would be straightforward. This model has also been mentioned in Ref. [54].

Of course, a singlet scalar DM can also have interactions with the Higgs boson, of the kind discussed in Sect. 3.2.1. However, in the spirit of the simplified model one usually ignores such interactions when studying the model described by Eq. (79).

By putting together the limits from the LHC, direct detection, thermal relic abundance and perturbativity of the coupling constant y , one finds that this model is rather constrained, but still some parameter space is available, for $m_\phi \gtrsim 1$ TeV and $m_\psi/m_\phi \lesssim 2$ (see Ref. [185] for more details).

Collider

At the LHC, it is possible to produce a pair of DM particles starting from two quarks with the mediator exchanged in the t -channel, and associated initial-state radiation. This would give the usual mono-jet ($\cancel{E}_T + j$) signal. In addition, if the mediator is light enough, a pair of mediators can be produced, with each of them subsequently decaying into DM and a quark, thus producing an \cancel{E}_T signal in association with 2 or more jets. One can therefore combine these two kinds of strategies to improve the discovery potential.

Notice that, since the mediator carries color and EW charges, the mediator pair-production can proceed either by DM exchange or by direct QCD and EW Drell-Yan production (see Refs. [188, 189] for experimental results on vector-like quark searches).

For mediator masses M_ψ of the same order as m_ϕ , the current LHC constraints imply $m_\phi \gtrsim 1$ TeV, but the bounds gets weaker as the mediator mass gets higher [185].

DM self-annihilation

The main tree-level process for DM self-annihilations is $\phi\phi \rightarrow \bar{q}q$, via t -channel exchange of the mediator ψ . This is the relevant process to be considered for indirect DM searches. The thermally-averaged self-annihilation cross section reads [185, 187]

$$\langle\sigma v_{\text{rel}}\rangle(\phi\phi \rightarrow \bar{q}q) = \frac{3y^4}{4\pi} \frac{1}{m_\phi^2 (1+r^2)^2} \left[\frac{m_q^2}{m_\phi^2} \left(1 - \frac{2}{3} \frac{1+2r^2}{(1+r^2)^2} v^2 \right) + \frac{v^4}{15(1+r^2)^2} \right] \quad (80)$$

with $r \equiv m_\psi/m_\phi > 1$. Notice the d -wave suppression v^4 , in the case of massless final state particles $m_q = 0$, peculiar to real scalar annihilations, and in contrast with the well-known p -wave suppression at work when the annihilating particles are Majorana fermions.

The processes of Virtual Internal Bremsstrahlung (radiation of a gluon from the t -channel mediator line), or the loop-induced annihilation of $\phi\phi \rightarrow gg$ are able to lift the velocity suppression and open up potentially sizeable contributions to the annihilation cross sections. In particular, the one-loop process contributes as $\sigma v \sim r^{-4}$ (but without m_q suppression) while the internal Bremsstrahlung contributes as $\sigma v \sim r^{-8}$.

So, for mediator masses sufficiently close to the DM particle (r close to 1) these higher-order contributions are able to overcome the tree-level process and dominate the annihilation cross section. However, when the mediator and DM mass are very close, it is also necessary to take into account the effects of co-annihilations (e.g. $\psi\psi \rightarrow \bar{q}q$) in the early universe.

As for the general treatment of the annihilations of two particles carrying color, the non-perturbative Sommerfeld effects may play an important role, see Refs. [114, 179, 185].

DM scattering on nucleons

In this model, the DM scattering on nucleons can proceed by tree-level fundamental interactions of DM with quarks (via exchange of ψ), or by loop-induced interactions of DM with gluons. In the former case, integrating out the heavy mediator ψ leads to effective interactions proportional to the quark mass operator and a twist-2 operator

$$\mathcal{L}_{\text{eff},1} \propto m_q \phi^2 \bar{q}q, \quad (81)$$

$$\mathcal{L}_{\text{eff},2} \propto \frac{i}{2} (\partial_\mu \phi) (\partial_\nu \phi) [\bar{q} \gamma^\mu \partial^\nu q + \bar{q} \gamma^\nu \partial^\mu q - (1/2) g^{\mu\nu} \bar{q} \not{d} q,] \quad (82)$$

while in the latter case,

$$\mathcal{L}_{\text{eff},3} \propto \frac{\alpha_s}{\pi} \phi^2 \text{Tr}[G_{\mu\nu} G^{\mu\nu}]. \quad (83)$$

The corresponding spin-independent DM-nucleon scattering cross section can be found using Eq. (20), with coefficient [185, 190]

$$c^N = \frac{y^2}{m_\phi^2} \left[\frac{2r^2-1}{4(r^2-1)^2} f_q^{(N)} + \frac{3}{4} (q_2^{(N)} + \bar{q}_2^{(N)}) - \frac{8}{9} \frac{y^2}{24(r^2-1)} f_g^{(N)} \right] \quad (84)$$

where $q_2^{(N)}, \bar{q}_2^{(N)}$ are the second moments of the PDFs of the parton q in the nucleon N , the first term comes from $\mathcal{L}_{\text{eff},1}$, the second term from $\mathcal{L}_{\text{eff},2}$ and the last term from the perturbative short-distance contribution from $\mathcal{L}_{\text{eff},3}$, where loop momenta are of the order of the DM mass.

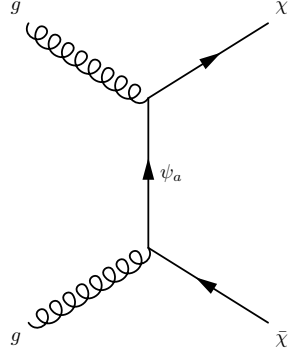


Fig. 8: Diagram for DM pair production in $\frac{1}{2}t\frac{1}{2}$ model.

3.3.2 Fermion DM, t -channel ($\frac{1}{2}t\frac{1}{2}$ model)

In the case of fermionic DM with a fermion mediator exchanged in the t -channel, the LHC production can be initiated by two gluons (see tree-level diagram in Fig. 8). The fermion DM cannot be colored, so the mediator needs to be a fermion octet (gluino-like) particle ψ^a of mass M .

The operators appearing at the lowest order in the Lagrangian of the model are

$$\mathcal{L}_{\frac{1}{2}t\frac{1}{2}} \supset \bar{\psi}^a (iD_\mu - M) \psi^a + \frac{1}{\Lambda} G_{\mu\nu}^a (\bar{\psi}^a \sigma^{\mu\nu} \chi + \text{h.c.}) \quad (85)$$

where D_μ is the covariant derivative involving the gluon field and the dimension-5 operator is of the form of a chromomagnetic dipole operator (resembling the gluino-gluon-bino interaction in SUSY).

Extensive searches are performed for this kind of mediator, driven by the interest in SUSY models. Limits from direct QCD production of gluino-like mediators decaying to two gluons and two DM particles tell us that the mediator must be heavier than about 1150 GeV (95% CL) for DM masses below 100 GeV [191].

However, apart from the direct mediator searches, no analyses have been performed to study the fermion octet in the context of a simplified model with a DM particle, to our knowledge. Of course, the dimension-5 interaction in Eq. (85) would lead to rather weak signals at LHC. But a careful study of this model, also in view of possible future colliders, would be interesting.

3.4 Vector Mediator

With a vector mediator, it is possible to produce a DM pair from an initial state of two quarks by exchanging the mediator in the s -channel, with DM being a scalar ($1s0$ model) or a fermion ($1s\frac{1}{2}$ model), or in the t -channel, with fermion DM ($1t\frac{1}{2}$ model).

We will consider the vector mediator as having an explicit mass, without trying to justify it from a more complete UV theory, following the philosophy behind simplified models. It is assumed that there exists some UV completion that can avoid problems of gauge invariance,

anomaly cancellation and mass generation; and importantly, that the phenomenology is independent of the UV completion. However, care must be taken, since this is not always the case. Some choices of parameters within simplified models can be pathological, such that no fully consistent UV completion exists. This is the case for a fully axial-vector model, where the model violates gauge invariance unless the SM particles also couple to the mediator via a vector coupling [192]. This can lead to unphysical signals in regions where the model violates perturbative unitarity [115, 193–195].

3.4.1 Scalar DM, *s*-channel (1s0 model)

For a complex scalar DM ϕ of mass m_ϕ coupled to the vector mediator V_μ of mass M_V , the Lagrangian of the model is given by

$$\mathcal{L}_{1s0} \supset -V^\mu \left[g_\phi \left[\phi^* (i\partial_\mu \phi) - \phi (i\partial_\mu \phi^*) \right] + \sum_f \bar{f} \gamma_\mu (g_f^V + g_f^A \gamma^5) f \right], \quad (86)$$

where the sum over f extends to all SM fermions.

The couplings $g_f^{V,A}$ need to be flavor independent in order to respect MFV hypothesis. It is customary in the literature to reduce the number of free parameters by considering only the limiting cases of a “purely vector” ($g_i^A = 0$) or a “purely axial” ($g_i^V = 0$) mediator.

Collider

The collider phenomenology of this class of models is crucially dependent on the leading decay channels of the vector mediator, provided they are kinematically accessible. The decay width of V to SM fermions f , with color number $N_c(f)$, is given by

$$\Gamma(V \rightarrow \bar{f}f) = N_c(f) \frac{M_V}{12\pi} \sqrt{1 - \frac{4m_f^2}{M_V^2}} \left[|g_f^V|^2 \left(1 + \frac{2m_f^2}{M_V^2} \right) + |g_f^A|^2 \left(1 - \frac{4m_f^2}{M_V^2} \right) \right], \quad (87)$$

while the (invisible) decay width to DM particles is

$$\Gamma(V \rightarrow \phi\phi) = \frac{g_\phi^2 M_V}{48\pi} \left(1 - \frac{4m_\phi^2}{M_V^2} \right)^{3/2}. \quad (88)$$

Roughly speaking, if invisible decays dominate ($V \rightarrow \phi\phi$), we expect the collider phenomenology to be driven by MET searches (e.g. mono-jet); conversely, if the mediator predominantly decays to SM fermions, the best search strategy would be the heavy resonances (e.g. di-jets [193] or di-leptons, although the latter case is highly constrained [88, 196]).

Further constraints arise from requiring a particle interpretation of the mediator (narrow-width approximation): $\Gamma_V/M_V < 1$.

DM self-annihilation

The DM self-annihilation cross section, to be used for relic density calculations or for indirect detection, is

$$\langle \sigma v_{\text{rel}} \rangle (\phi\phi \rightarrow f\bar{f}) = N_c(f) \frac{g_\phi^2}{6\pi} \frac{m_\phi^2 \sqrt{1 - \frac{m_f^2}{m_\phi^2}}}{(4m_\phi^2 - M_V^2)^2} \left[|g_f^V|^2 \left(1 + \frac{1}{2} \frac{m_f^2}{m_\phi^2} \right) + |g_f^A|^2 \left(1 - \frac{m_f^2}{m_\phi^2} \right) \right] v_{\text{rel}}^2, \quad (89)$$

which is in *p*-wave.

DM scattering on nucleons

At low-energies, the DM-nucleon scattering is described by the effective operator

$$\begin{aligned}\mathcal{L}_{\text{eff}} &= \sum_q \frac{g_\phi}{M_V^2} [\phi^*(i\partial_\mu \phi) - \phi(i\partial_\mu \phi^*)] [\bar{q} \gamma^\mu (g_q^V + g_q^A \gamma^5) q] \\ &\simeq \sum_q \frac{g_\phi g_q^V}{M_V^2} [\phi^*(i\partial_\mu \phi) - \phi(i\partial_\mu \phi^*)] [\bar{q} \gamma^\mu q]\end{aligned}\quad (90)$$

where the axial contribution has been neglected as it gives rise to a subdominant spin-dependent scattering cross section. The spin-independent component of the cross section can be found using Eq. (20), with coefficients (cf. Table 8)

$$c^p = \frac{1}{M_V^2} g_\phi (2g_u^V + g_d^V), \quad c^n = \frac{1}{M_V^2} g_\phi (2g_d^V + g_u^V). \quad (91)$$

3.4.2 Fermion DM, *s*-channel ($1s_{\frac{1}{2}}$ model)

The Lagrangian of the model is given by

$$\mathcal{L}_{1s_{\frac{1}{2}}} \supset -V^\mu \left[\bar{\chi} \gamma_\mu (g_\chi^V + g_\chi^A \gamma^5) \chi + \sum_f \bar{f} \gamma_\mu (g_f^V + g_f^A \gamma^5) f \right], \quad (92)$$

where the sum over f extends to all SM fermions. If χ is Majorana, the vector bilinears vanish identically, so $g_\chi^V = 0$.

The MFV hypothesis imposes the couplings $g_f^{V,A}$ to be flavor independent. In the most general case, there are several model parameters, therefore a “purely vector” ($g_i^A = 0$) or a “purely axial” ($g_i^V = 0$) mediator is often assumed in the literature.

Collider

The collider phenomenology of the mediator is the same as the one already discussed for the $1s0$ model, except that the invisible width of the mediator is now given by the same expression as the decay to SM fermions Eq. (87) with the index f replaced by the index χ and $N_c(\chi) = 1$.

DM self-annihilation

The dominant (*s*-wave) contribution to the DM self annihilation cross-section is

$$\begin{aligned}\langle \sigma v_{\text{rel}} \rangle (\chi \chi \rightarrow f \bar{f}) &= \frac{N_c(f)}{2\pi} \frac{m_\chi^2 \sqrt{1 - \frac{m_f^2}{m_\chi^2}}}{(4m_\chi^2 - M_V^2)^2} \left\{ |g_\chi^V|^2 \left[|g_f^V|^2 \left(2 + \frac{m_f^2}{m_\chi^2} \right) + 2|g_f^A|^2 \left(1 - \frac{m_f^2}{m_\chi^2} \right) \right] \right. \\ &\quad \left. + |g_\chi^A|^2 |g_f^A|^2 \frac{m_f^2}{m_\chi^2} \left(1 - \frac{4m_\chi^2}{m_V^2} \right)^2 \right\},\end{aligned}\quad (93)$$

where the term proportional to $|g_\chi^A|^2 |g_f^V|^2$ is absent here because it appears only at the level of *p*-wave.

DM scattering on nucleons

In the low-energy limit, the effective interactions relevant for DM-nucleon scatterings are

$$\mathcal{L}_{\text{eff}} = \sum_q \frac{1}{M_V^2} \left[\bar{\chi} \gamma_\mu (g_\chi^V + g_\chi^A \gamma^5) \chi \right] \left[\bar{q} \gamma^\mu (g_q^V + g_q^A \gamma^5) q \right]$$

The $g_\chi^V g_q^V$ terms lead to a SI cross section, while the purely axial terms proportional to $g_\chi^A g_q^A$ lead to SD scattering. The cross terms $g_\chi^V g_q^A, g_\chi^A g_q^V$ give cross sections suppressed by either the DM velocity or the momentum, so they are subdominant and can be neglected. The spin-independent component of the cross-section is given by Eq. (20) with coefficients (cf. Table 6)

$$c^p = \frac{1}{M_V^2} g_\chi^V (2g_u^V + g_d^V), \quad c^n = \frac{1}{M_V^2} g_\chi^V (2g_d^V + g_u^V), \quad (94)$$

and the spin-dependent component by Eq. (21) with coefficient (cf. Table 6)

$$c^N = \frac{1}{M_V^2} \sum_{q=u,d,s} g_\chi^A g_q^A \Delta_q^{(N)}, \quad (95)$$

where sample values for $\Delta_q^{(N)}$ are given in Table 7.

■ CASE STUDY 3: Z AS MEDIATOR

The SM Z boson itself may serve as a vector mediator, rather than a speculative particle. In this case, the couplings $g_f^{V,A}$ of the Z boson to SM fermions are well-known: $g_V = (g_2/\cos\theta_W)(1/4 - (2/3)\sin^2\theta_W)$, $g_A = -g_2/(4\cos\theta_W)$ for up-type quarks, and $g_V = (g_2/\cos\theta_W)(-1/4 + (1/3)\sin^2\theta_W)$, $g_A = g_2/(4\cos\theta_W)$ for down-type quarks, where g_2 is the $SU(2)_L$ gauge coupling and θ_W is the weak mixing angle.

The Lagrangian has the same form as that of a generic vector mediator Eq. (86) for scalar DM or Eq. (92) for fermion DM, therefore all the results listed in Sections 3.4.1 and 3.4.2 apply, except that the Z couplings to fermions $g_f^{V,A}$ are known.

Let us summarize the main points of the analysis carried out in Ref. [114], to which we refer the reader for further details. In the mass regime where Z-decays to DM are kinematically allowed ($m_\chi < M_Z/2$), the experimental constraint on the Z invisible width $\Gamma_{Z,\text{inv}} \lesssim 2$ MeV gives $g_\phi \lesssim 0.08(g_2/\cos\theta_W)$ and $g_\chi^{V,A} \lesssim 0.04(g_2/\cos\theta_W)$.

The opposite mass regime $m_\chi > M_Z/2$ is not significantly constrained by collider data with respect to the much stronger constraints coming from direct detection.

Indeed, direct detection experiments (currently dominated by LUX results), place quite strong limits on $g_\chi^V, g_\phi \lesssim 10^{-3}(g_2/\cos\theta_W)$ for DM masses around 100 GeV, while the spin-dependent interactions lead to a milder bound on $g_\chi^A \lesssim 0.3(g_2/\cos\theta_W)$ for DM mass around 100 GeV.

As far as the thermal relic density is concerned, a scalar thermal DM candidate accounting for 100% of the DM abundance is ruled out, for $m_\phi \lesssim$ TeV. As for fermion DM, the pure vector case ($g_\chi^A = 0$) is still compatible with direct detection and relic abundance for DM masses above about 1 TeV (and near the resonance region $m_\chi \simeq M_Z/2$), while a thermal DM candidate with pure axial couplings to the Z ($g_\chi^V = 0$) is still viable in most of the parameter space with $m_\chi > M_Z/2$.

However, It should be kept in mind that the conclusions drawn above are only valid within the simple model described by the SM plus the DM particle; new physics particles and interactions at the weak scale can have a big impact on the bounds from relic density.

■ CASE STUDY 4: A SUSY-INSPIRED EXAMPLE, SINGLET-DOUBLET DM

A different possibility is to allow mixing between an EW singlet and an EW doublet as a mechanism to generate interactions between the dark and the visible sectors [197–200]. Such a situation is also interesting because it can be realized in SUSY with a bino-higgsino mixing, in the decoupling limit where the masses of the scalar superpartners and of the wino are much larger than M_1 and $|\mu|$.

The particle content of the model consists of a fermion singlet χ and two fermion doublets $\Psi_1 = (\Psi_1^0, \Psi_1^-)^T$ and $\Psi_2 = (\Psi_2^+, \Psi_2^0)^T$, with opposite hypercharges. There is a discrete Z_2 symmetry under which χ, Ψ_1, Ψ_2 are odd while the SM particles are even. The Lagrangian describing the interactions is given by

$$\mathcal{L} = \bar{\chi}(i\partial) \chi + \sum_{i=1,2} \bar{\Psi}_i(i\partial) \Psi_i - \frac{1}{2}(\chi, \Psi_1, \Psi_2) \mathcal{M}(\chi, \Psi_1, \Psi_2)^T \quad (96)$$

where D_μ is the covariant derivative and the mass matrix is

$$\mathcal{M} = \begin{pmatrix} m_S & y_1 \frac{v}{\sqrt{2}} & y_2 \frac{v}{\sqrt{2}} \\ y_1 \frac{v}{\sqrt{2}} & 0 & m_D \\ y_2 \frac{v}{\sqrt{2}} & m_D & 0 \end{pmatrix} \quad (97)$$

with m_S, m_D the mass parameters for the singlet and doublet, respectively. The off-diagonal singlet-doublet mixing terms arise from interaction terms with the Higgs (after EW symmetry breaking) of the kind $-\chi(y_1 H \Psi_1 + y_2 H^\dagger \Psi_2) + \text{h.c.}$.

The diagonalization of the mass matrix via the unitary matrix U performs the shift to the mass-eigenstates basis where the physical spectrum of the model becomes apparent: 2 charged states χ^\pm and 3 neutral states $\chi_{1,2,3}$ such as

$$\begin{pmatrix} \chi_1 \\ \chi_2 \\ \chi_3 \end{pmatrix} = U \begin{pmatrix} \chi \\ \Psi_1 \\ \Psi_2 \end{pmatrix} \quad (98)$$

with the lightest neutral state χ playing the role of the DM particle.

In the language of SUSY, the lightest neutralino coming from the mixing with bino-higgsino states is the DM. One can recover the SUSY situation with the following identifications: $m_S = M_1, m_D = |\mu|$, $y_1 = -\cos\beta g_1/\sqrt{2}$ and $y_2 = \sin\beta g_1/\sqrt{2}$, where g_1 is the $U(1)_Y$ gauge coupling and β is the misalignment angle between the VEVs of H_u and H_d : $\tan\beta = v_u/v_d$.

In the mass-eigenstates basis it is also easy to read the interactions between the new states and the SM bosons (physical Higgs h and Z, W^\pm)

$$\begin{aligned} \mathcal{L} \supset & -h\bar{\chi}_i(\Re(c_{ij}^h)\gamma^5 + \Im(c_{ij}^h)\gamma^5)\chi_j - Z_\mu\bar{\chi}_i\gamma^\mu(\Im(c_{ij}^Z) - \Re(c_{ij}^Z)\gamma^5)\chi_j \\ & - \frac{g_2}{2\sqrt{2}} \left((U_{i3} - U_{i2}^*)W_\mu^-\bar{\chi}_i\gamma^\mu\chi^+ - (U_{i3} + U_{i2}^*)W_\mu^-\bar{\chi}_i\gamma^\mu\gamma^5\chi^+ + \text{h.c.} \right), \end{aligned} \quad (99)$$

with $i, j = 1, 3$ and where the couplings to h and Z are

$$c_{ij}^h = \frac{1}{\sqrt{2}}(y_1 U_{i2} U_{j1} + y_2 U_{i3} U_{j1}), \quad c_{ij}^Z = \frac{g_2}{4\cos\theta_W}(U_{i3} U_{j3}^* - U_{i2} U_{j2}^*) \quad (100)$$

Notice that the DM coupling to Z boson c_{11}^Z has no imaginary part, leading to a purely axial-vector interaction, and therefore to a spin-suppressed cross section of DM with nucleons, arising from a mix of operators $\mathcal{O}_4^{\text{NR}}$, $\mathcal{O}_8^{\text{NR}}$ and $\mathcal{O}_9^{\text{NR}}$.

As we see, this model generates a somewhat hybrid situation given by a combination of $0s_{\frac{1}{2}}^1$ and $1s_{\frac{1}{2}}^1$ models, where the mediation from the dark to the visible sector is provided by both the Higgs and the W, Z bosons.

The self-annihilations of DM proceed via s -channel exchange of a Higgs or a Z boson, to a fermion-antifermion final state. But it is also possible for DM to exchange a χ_i or a χ^{\pm} in the t -channel to lead to hh, ZZ, WW final states.

If kinematically open, the interactions in Eq. (99) contribute to the invisible width of h and Z , as

$$\Gamma(h \rightarrow \chi_1 \chi_1) = \frac{|c_{11}^h|^2}{4\pi} m_h \left(1 - \frac{4m_{\chi_1}^2}{m_h^2}\right)^{3/2} \quad (101)$$

$$\Gamma(h \rightarrow \chi_1 \chi_1) = \frac{|c_{11}^Z|^2}{6\pi} m_Z \left(1 - \frac{4m_{\chi_1}^2}{m_Z^2}\right)^{3/2} \quad (102)$$

and the limits on these widths can be used to place bounds on the parameter space

At the LHC, there is a richer phenomenology due to the presence of more (also charged) states. Indeed, in addition to a top-loop-induced gluon fusion process $gg \rightarrow \chi_i \chi_j$ there is also a Drell-Yan-type production via EW bosons which opens production modes of the kind $q\bar{q} \rightarrow \chi_i \chi_j, \chi^+ \chi^-$ (Z -exchange) or $q\bar{q} \rightarrow \chi_i \chi^{\pm}$ (W -exchange). The further decay of the heavier part of the spectrum $\chi^{\pm}, \chi_{2,3}$ to the lightest DM particle χ_1 involves further gauge boson radiation with the possibility of lepton-rich final states (such as $2\ell + \cancel{E}_T$ or $3\ell + \cancel{E}_T$), offering clean handles for searches.

3.4.3 Fermion DM, t -channel ($1t_{\frac{1}{2}}$ model)

At tree-level, it is possible to produce a pair of fermion-DM particles by two initial-state quarks exchanging a vector mediator in the t -channel. In order to preserve the color-, flavor- and charge-neutrality of DM, the mediator should carry flavor, color and electric charge. In particular, it must be a color-triplet.

The corresponding LHC phenomenology has some similarities with that of the $0t_{\frac{1}{2}}$ model (squark-like mediator), as similar diagrams contribute to the mono-jet signal. But on the other hand, the direct production of the mediator would be different, because of its quantum numbers under $SU(3)_c$ and Lorentz.

As for the $\frac{1}{2}t_{\frac{1}{2}}$ model, to our knowledge there have been no analyses of the phenomenology of a color-triplet mediator in the context of a simplified model with a DM particle.

4 Conclusions

In this review we have discussed and compared two important frameworks to describe the phenomenology of particle (WIMP) DM and simultaneously keep the number of parameters as minimal as possible: the EFT approach and simplified models.

Both of these approaches have virtues and drawbacks, but it is now clear that the use of EFTs in collider searches for DM suffers from important limitations. Therefore, the currently best available candidate for providing a simple common language to describe the different aspects of DM phenomenology (collider, direct and indirect searches) turns out to be simplified models.

Of course, this does not mean that alternative approaches are not possible or not interesting, and by no means this state-of-the-art review should be regarded as exhaustive. The subject is currently rapidly changing and expanding, in response to an ever-increasing interest in the problem of the identification of DM.

We have provided an overview of the subject of EFTs for DM searches, spelling out the theoretical issues involved in its use but also its advantages. For each effective operator, we also highlighted how to make the connection among the different search strategies.

In the Section dedicated to simplified models, we provided a general classification of the models, and proposed a simple nomenclature system for them (cf. Table 9). Wherever available, we collected the main results regarding the application of the simplified model to describe the phenomenology of DM production at collider, DM self-annihilations and DM scattering with nuclei. We also emphasized, to the best of our knowledge, which models have been least addressed in the literature, encouraging work to fill these gaps.

By interpreting the results of the different DM searches within a single theoretical framework, such as the one provided by simplified models, it is possible to dramatically increase the discovery potential and make the discovery of DM more accessible.

Acknowledgements We are grateful to our collaborators Giorgio Busoni, Johanna Gramling, Enrico Morgante and Antonio Riotto, with whom we co-authored papers on this subject. We also thank the members of the LHC Dark Matter Working Group for very interesting discussions.

References

1. **Planck** Collaboration, P. A. R. Ade et al., *Planck 2013 results. XVI. Cosmological parameters*, *Astron. Astrophys.* **571** (2014) A16, [[arXiv:1303.5076](https://arxiv.org/abs/1303.5076)].
2. A. Birkedal, K. Matchev, and M. Perelstein, *Dark matter at colliders: A Model independent approach*, *Phys. Rev.* **D70** (2004) 077701, [[hep-ph/0403004](https://arxiv.org/abs/hep-ph/0403004)].
3. J. L. Feng, S. Su, and F. Takayama, *Lower limit on dark matter production at the large hadron collider*, *Phys. Rev. Lett.* **96** (2006) 151802, [[hep-ph/0503117](https://arxiv.org/abs/hep-ph/0503117)].
4. M. Beltran, D. Hooper, E. W. Kolb, and Z. C. Krusberg, *Deducing the nature of dark matter from direct and indirect detection experiments in the absence of collider signatures of new physics*, *Phys. Rev.* **D80** (2009) 043509, [[arXiv:0808.3384](https://arxiv.org/abs/0808.3384)].
5. Q.-H. Cao, C.-R. Chen, C. S. Li, and H. Zhang, *Effective Dark Matter Model: Relic density, CDMS II, Fermi LAT and LHC*, *JHEP* **08** (2011) 018, [[arXiv:0912.4511](https://arxiv.org/abs/0912.4511)].
6. M. Beltran, D. Hooper, E. W. Kolb, Z. A. C. Krusberg, and T. M. P. Tait, *Maverick dark matter at colliders*, *JHEP* **09** (2010) 037, [[arXiv:1002.4137](https://arxiv.org/abs/1002.4137)].
7. P. Agrawal, Z. Chacko, C. Kilic, and R. K. Mishra, *A Classification of Dark Matter Candidates with Primarily Spin-Dependent Interactions with Matter*, [arXiv:1003.1912](https://arxiv.org/abs/1003.1912).
8. J. Goodman, M. Ibe, A. Rajaraman, W. Shepherd, T. M. P. Tait, and H.-B. Yu, *Constraints on Light Majorana dark Matter from Colliders*, *Phys. Lett.* **B695** (2011) 185–188, [[arXiv:1005.1286](https://arxiv.org/abs/1005.1286)].
9. Y. Bai, P. J. Fox, and R. Harnik, *The Tevatron at the Frontier of Dark Matter Direct Detection*, *JHEP* **12** (2010) 048, [[arXiv:1005.3797](https://arxiv.org/abs/1005.3797)].
10. J. Fan, M. Reece, and L.-T. Wang, *Non-relativistic effective theory of dark matter direct detection*, *JCAP* **1011** (2010) 042, [[arXiv:1008.1591](https://arxiv.org/abs/1008.1591)].

11. J. Goodman, M. Ibe, A. Rajaraman, W. Shepherd, T. M. P. Tait, and H.-B. Yu, *Constraints on Dark Matter from Colliders*, *Phys. Rev.* **D82** (2010) 116010, [[arXiv:1008.1783](https://arxiv.org/abs/1008.1783)].
12. J. Goodman, M. Ibe, A. Rajaraman, W. Shepherd, T. M. P. Tait, and H.-B. Yu, *Gamma Ray Line Constraints on Effective Theories of Dark Matter*, *Nucl. Phys.* **B844** (2011) 55–68, [[arXiv:1009.0008](https://arxiv.org/abs/1009.0008)].
13. K. Cheung, P.-Y. Tseng, and T.-C. Yuan, *Cosmic Antiproton Constraints on Effective Interactions of the Dark Matter*, *JCAP* **1101** (2011) 004, [[arXiv:1011.2310](https://arxiv.org/abs/1011.2310)].
14. J.-M. Zheng, Z.-H. Yu, J.-W. Shao, X.-J. Bi, Z. Li, and H.-H. Zhang, *Constraining the interaction strength between dark matter and visible matter: I. fermionic dark matter*, *Nucl. Phys.* **B854** (2012) 350–374, [[arXiv:1012.2022](https://arxiv.org/abs/1012.2022)].
15. P. J. Fox, R. Harnik, J. Kopp, and Y. Tsai, *LEP Shines Light on Dark Matter*, *Phys. Rev.* **D84** (2011) 014028, [[arXiv:1103.0240](https://arxiv.org/abs/1103.0240)].
16. J.-F. Fortin and T. M. P. Tait, *Collider Constraints on Dipole-Interacting Dark Matter*, *Phys. Rev.* **D85** (2012) 063506, [[arXiv:1103.3289](https://arxiv.org/abs/1103.3289)].
17. M. R. Buckley, *Asymmetric Dark Matter and Effective Operators*, *Phys. Rev.* **D84** (2011) 043510, [[arXiv:1104.1429](https://arxiv.org/abs/1104.1429)].
18. K. Cheung, P.-Y. Tseng, and T.-C. Yuan, *Gamma-ray Constraints on Effective Interactions of the Dark Matter*, *JCAP* **1106** (2011) 023, [[arXiv:1104.5329](https://arxiv.org/abs/1104.5329)].
19. J. Wang, C. S. Li, D. Y. Shao, and H. Zhang, *Next-to-leading order QCD predictions for the signal of Dark Matter and photon associated production at the LHC*, *Phys. Rev.* **D84** (2011) 075011, [[arXiv:1107.2048](https://arxiv.org/abs/1107.2048)].
20. M. T. Frandsen, F. Kahlhoefer, S. Sarkar, and K. Schmidt-Hoberg, *Direct detection of dark matter in models with a light Z'*, *JHEP* **09** (2011) 128, [[arXiv:1107.2118](https://arxiv.org/abs/1107.2118)].
21. A. Rajaraman, W. Shepherd, T. M. P. Tait, and A. M. Wijangco, *LHC Bounds on Interactions of Dark Matter*, *Phys. Rev.* **D84** (2011) 095013, [[arXiv:1108.1196](https://arxiv.org/abs/1108.1196)].
22. G. F. Giudice, B. Gripaios, and R. Mahbubani, *Counting dark matter particles in LHC events*, *Phys. Rev.* **D85** (2012) 075019, [[arXiv:1108.1800](https://arxiv.org/abs/1108.1800)].
23. P. Agrawal, S. Blanchet, Z. Chacko, and C. Kilic, *Flavored Dark Matter, and Its Implications for Direct Detection and Colliders*, *Phys. Rev.* **D86** (2012) 055002, [[arXiv:1109.3516](https://arxiv.org/abs/1109.3516)].
24. P. J. Fox, R. Harnik, J. Kopp, and Y. Tsai, *Missing Energy Signatures of Dark Matter at the LHC*, *Phys. Rev.* **D85** (2012) 056011, [[arXiv:1109.4398](https://arxiv.org/abs/1109.4398)].
25. J. Goodman and W. Shepherd, *LHC Bounds on UV-Complete Models of Dark Matter*, [arXiv:1111.2359](https://arxiv.org/abs/1111.2359).
26. K. N. Abazajian, P. Agrawal, Z. Chacko, and C. Kilic, *Lower Limits on the Strengths of Gamma Ray Lines from WIMP Dark Matter Annihilation*, *Phys. Rev.* **D85** (2012) 123543, [[arXiv:1111.2835](https://arxiv.org/abs/1111.2835)].
27. I. M. Shoemaker and L. Vecchi, *Unitarity and Monojet Bounds on Models for DAMA, CoGeNT, and CRESST-II*, *Phys. Rev.* **D86** (2012) 015023, [[arXiv:1112.5457](https://arxiv.org/abs/1112.5457)].
28. R. Ding and Y. Liao, *Spin 3/2 Particle as a Dark Matter Candidate: an Effective Field Theory Approach*, *JHEP* **04** (2012) 054, [[arXiv:1201.0506](https://arxiv.org/abs/1201.0506)].
29. K. Cheung, P.-Y. Tseng, Y.-L. S. Tsai, and T.-C. Yuan, *Global Constraints on Effective Dark Matter Interactions: Relic Density, Direct Detection, Indirect Detection, and Collider*, *JCAP* **1205** (2012) 001, [[arXiv:1201.3402](https://arxiv.org/abs/1201.3402)].
30. H. An, X. Ji, and L.-T. Wang, *Light Dark Matter and Z' Dark Force at Colliders*, *JHEP* **07** (2012) 182, [[arXiv:1202.2894](https://arxiv.org/abs/1202.2894)].
31. P. J. Fox, R. Harnik, R. Primulando, and C.-T. Yu, *Taking a Razor to Dark Matter Parameter Space at the LHC*, *Phys. Rev.* **D86** (2012) 015010, [[arXiv:1203.1662](https://arxiv.org/abs/1203.1662)].

32. A. L. Fitzpatrick, W. Haxton, E. Katz, N. Lubbers, and Y. Xu, *The Effective Field Theory of Dark Matter Direct Detection*, *JCAP* **1302** (2013) 004, [[arXiv:1203.3542](https://arxiv.org/abs/1203.3542)].

33. M. T. Frandsen, F. Kahlhoefer, A. Preston, S. Sarkar, and K. Schmidt-Hoberg, *LHC and Tevatron Bounds on the Dark Matter Direct Detection Cross-Section for Vector Mediators*, *JHEP* **07** (2012) 123, [[arXiv:1204.3839](https://arxiv.org/abs/1204.3839)].

34. V. Barger, W.-Y. Keung, D. Marfatia, and P.-Y. Tseng, *Dipole Moment Dark Matter at the LHC*, *Phys. Lett.* **B717** (2014) 219–223, [[arXiv:1206.0640](https://arxiv.org/abs/1206.0640)].

35. M. Garny, A. Ibarra, M. Pato, and S. Vogl, *Closing in on mass-degenerate dark matter scenarios with antiprotons and direct detection*, *JCAP* **1211** (2012) 017, [[arXiv:1207.1431](https://arxiv.org/abs/1207.1431)].

36. M. T. Frandsen, U. Haisch, F. Kahlhoefer, P. Mertsch, and K. Schmidt-Hoberg, *Loop-induced dark matter direct detection signals from gamma-ray lines*, *JCAP* **1210** (2012) 033, [[arXiv:1207.3971](https://arxiv.org/abs/1207.3971)].

37. Y. Bai and T. M. P. Tait, *Searches with Mono-Leptons*, *Phys. Lett.* **B723** (2013) 384–387, [[arXiv:1208.4361](https://arxiv.org/abs/1208.4361)].

38. U. Haisch, F. Kahlhoefer, and J. Unwin, *The impact of heavy-quark loops on LHC dark matter searches*, *JHEP* **07** (2013) 125, [[arXiv:1208.4605](https://arxiv.org/abs/1208.4605)].

39. N. F. Bell, J. B. Dent, A. J. Galea, T. D. Jacques, L. M. Krauss, and T. J. Weiler, *Searching for Dark Matter at the LHC with a Mono-Z*, *Phys. Rev.* **D86** (2012) 096011, [[arXiv:1209.0231](https://arxiv.org/abs/1209.0231)].

40. F. P. Huang, C. S. Li, J. Wang, and D. Y. Shao, *Searching for the signal of dark matter and photon associated production at the LHC beyond leading order*, *Phys. Rev.* **D87** (2013) 094018, [[arXiv:1210.0195](https://arxiv.org/abs/1210.0195)].

41. R. C. Cotta, J. L. Hewett, M. P. Le, and T. G. Rizzo, *Bounds on Dark Matter Interactions with Electroweak Gauge Bosons*, *Phys. Rev.* **D88** (2013) 116009, [[arXiv:1210.0525](https://arxiv.org/abs/1210.0525)].

42. H. An, R. Huo, and L.-T. Wang, *Searching for Low Mass Dark Portal at the LHC*, *Phys. Dark Univ.* **2** (2013) 50–57, [[arXiv:1212.2221](https://arxiv.org/abs/1212.2221)].

43. L. M. Carpenter, A. Nelson, C. Shimmin, T. M. P. Tait, and D. Whiteson, *Collider searches for dark matter in events with a Z boson and missing energy*, *Phys. Rev.* **D87** (2013), no. 7 074005, [[arXiv:1212.3352](https://arxiv.org/abs/1212.3352)].

44. A. De Simone, A. Monin, A. Thamm, and A. Urbano, *On the effective operators for Dark Matter annihilations*, *JCAP* **1302** (2013) 039, [[arXiv:1301.1486](https://arxiv.org/abs/1301.1486)].

45. N. Zhou, D. Berge, and D. Whiteson, *Mono-everything: combined limits on dark matter production at colliders from multiple final states*, *Phys. Rev.* **D87** (2013), no. 9 095013, [[arXiv:1302.3619](https://arxiv.org/abs/1302.3619)].

46. H. Dreiner, D. Schmeier, and J. Tattersall, *Contact Interactions Probe Effective Dark Matter Models at the LHC*, *Europhys. Lett.* **102** (2013) 51001, [[arXiv:1303.3348](https://arxiv.org/abs/1303.3348)].

47. T. Lin, E. W. Kolb, and L.-T. Wang, *Probing dark matter couplings to top and bottom quarks at the LHC*, *Phys. Rev.* **D88** (2013), no. 6 063510, [[arXiv:1303.6638](https://arxiv.org/abs/1303.6638)].

48. H. M. Lee, M. Park, and V. Sanz, *Gravity-mediated (or Composite) Dark Matter*, *Eur. Phys. J.* **C74** (2014) 2715, [[arXiv:1306.4107](https://arxiv.org/abs/1306.4107)].

49. B. Bellazzini, M. Cliche, and P. Tanedo, *Effective theory of self-interacting dark matter*, *Phys. Rev.* **D88** (2013), no. 8 083506, [[arXiv:1307.1129](https://arxiv.org/abs/1307.1129)].

50. G. Busoni, A. De Simone, E. Morgante, and A. Riotto, *On the Validity of the Effective Field Theory for Dark Matter Searches at the LHC*, *Phys. Lett.* **B728** (2014) 412–421, [[arXiv:1307.2253](https://arxiv.org/abs/1307.2253)].

51. Z.-H. Yu, Q.-S. Yan, and P.-F. Yin, *Detecting interactions between dark matter and photons at high energy e^+e^- colliders*, *Phys. Rev.* **D88** (2013), no. 7 075015, [[arXiv:1307.5740](https://arxiv.org/abs/1307.5740)].

52. S. Profumo, W. Shepherd, and T. Tait, *Pitfalls of dark matter crossing symmetries*, *Phys. Rev.* **D88** (2013), no. 5 056018, [[arXiv:1307.6277](https://arxiv.org/abs/1307.6277)].

53. S. Chang, R. Edezhath, J. Hutchinson, and M. Luty, *Effective WIMPs*, *Phys. Rev.* **D89** (2014), no. 1 015011, [[arXiv:1307.8120](https://arxiv.org/abs/1307.8120)].

54. H. An, L.-T. Wang, and H. Zhang, *Dark matter with t -channel mediator: a simple step beyond contact interaction*, *Phys. Rev.* **D89** (2014), no. 11 115014, [[arXiv:1308.0592](https://arxiv.org/abs/1308.0592)].

55. Y. Bai and J. Berger, *Fermion Portal Dark Matter*, *JHEP* **11** (2013) 171, [[arXiv:1308.0612](https://arxiv.org/abs/1308.0612)].

56. A. DiFranzo, K. I. Nagao, A. Rajaraman, and T. M. P. Tait, *Simplified Models for Dark Matter Interacting with Quarks*, *JHEP* **11** (2013) 014, [[arXiv:1308.2679](https://arxiv.org/abs/1308.2679)]. [Erratum: *JHEP* 01, 162 (2014)].

57. O. Buchmueller, M. J. Dolan, and C. McCabe, *Beyond Effective Field Theory for Dark Matter Searches at the LHC*, *JHEP* **01** (2014) 025, [[arXiv:1308.6799](https://arxiv.org/abs/1308.6799)].

58. U. Haisch, F. Kahlhoefer, and E. Re, *QCD effects in mono-jet searches for dark matter*, *JHEP* **12** (2013) 007, [[arXiv:1310.4491](https://arxiv.org/abs/1310.4491)].

59. M. A. Fedderke, E. W. Kolb, T. Lin, and L.-T. Wang, *Gamma-ray constraints on dark-matter annihilation to electroweak gauge and Higgs bosons*, *JCAP* **1401** (2014), no. 01 001, [[arXiv:1310.6047](https://arxiv.org/abs/1310.6047)].

60. C. Cheung and D. Sanford, *Simplified Models of Mixed Dark Matter*, *JCAP* **1402** (2014) 011, [[arXiv:1311.5896](https://arxiv.org/abs/1311.5896)].

61. N. F. Bell, Y. Cai, and A. D. Medina, *Co-annihilating Dark Matter: Effective Operator Analysis and Collider Phenomenology*, *Phys. Rev.* **D89** (2014), no. 11 115001, [[arXiv:1311.6169](https://arxiv.org/abs/1311.6169)].

62. U. Haisch, A. Hibbs, and E. Re, *Determining the structure of dark-matter couplings at the LHC*, *Phys. Rev.* **D89** (2014) 034009, [[arXiv:1311.7131](https://arxiv.org/abs/1311.7131)].

63. M. B. Krauss, S. Morisi, W. Porod, and W. Winter, *Higher Dimensional Effective Operators for Direct Dark Matter Detection*, *JHEP* **02** (2014) 056, [[arXiv:1312.0009](https://arxiv.org/abs/1312.0009)].

64. G. Busoni, A. De Simone, J. Gramling, E. Morgante, and A. Riotto, *On the Validity of the Effective Field Theory for Dark Matter Searches at the LHC, Part II: Complete Analysis for the s -channel*, *JCAP* **1406** (2014) 060, [[arXiv:1402.1275](https://arxiv.org/abs/1402.1275)].

65. C. P. Burgess, M. Pospelov, and T. ter Veldhuis, *The Minimal model of nonbaryonic dark matter: A Singlet scalar*, *Nucl. Phys.* **B619** (2001) 709–728, [[hep-ph/0011335](https://arxiv.org/abs/hep-ph/0011335)].

66. H. Davoudiasl, R. Kitano, T. Li, and H. Murayama, *The New minimal standard model*, *Phys. Lett.* **B609** (2005) 117–123, [[hep-ph/0405097](https://arxiv.org/abs/hep-ph/0405097)].

67. B. Patt and F. Wilczek, *Higgs-field portal into hidden sectors*, [hep-ph/0605188](https://arxiv.org/abs/hep-ph/0605188).

68. S. Andreas, T. Hambye, and M. H. G. Tytgat, *WIMP dark matter, Higgs exchange and DAMA*, *JCAP* **0810** (2008) 034, [[arXiv:0808.0255](https://arxiv.org/abs/0808.0255)].

69. V. Barger, P. Langacker, M. McCaskey, M. Ramsey-Musolf, and G. Shaughnessy, *Complex Singlet Extension of the Standard Model*, *Phys. Rev.* **D79** (2009) 015018, [[arXiv:0811.0393](https://arxiv.org/abs/0811.0393)].

70. R. N. Lerner and J. McDonald, *Gauge singlet scalar as inflaton and thermal relic dark matter*, *Phys. Rev.* **D80** (2009) 123507, [[arXiv:0909.0520](https://arxiv.org/abs/0909.0520)].

71. X.-G. He, T. Li, X.-Q. Li, J. Tandean, and H.-C. Tsai, *The Simplest Dark-Matter Model, CDMS II Results, and Higgs Detection at LHC*, *Phys. Lett.* **B688** (2010)

332–336, [[arXiv:0912.4722](#)].

72. S. Kanemura, S. Matsumoto, T. Nabeshima, and N. Okada, *Can WIMP Dark Matter overcome the Nightmare Scenario?*, *Phys. Rev.* **D82** (2010) 055026, [[arXiv:1005.5651](#)].

73. V. Barger, Y. Gao, M. McCaskey, and G. Shaughnessy, *Light Higgs Boson, Light Dark Matter and Gamma Rays*, *Phys. Rev.* **D82** (2010) 095011, [[arXiv:1008.1796](#)].

74. A. Biswas and D. Majumdar, *The Real Gauge Singlet Scalar Extension of Standard Model: A Possible Candidate of Cold Dark Matter*, *Pramana* **80** (2013) 539–557, [[arXiv:1102.3024](#)].

75. C. Englert, T. Plehn, D. Zerwas, and P. M. Zerwas, *Exploring the Higgs portal*, *Phys. Lett.* **B703** (2011) 298–305, [[arXiv:1106.3097](#)].

76. Y. Mambrini, *Higgs searches and singlet scalar dark matter: Combined constraints from XENON 100 and the LHC*, *Phys. Rev.* **D84** (2011) 115017, [[arXiv:1108.0671](#)].

77. M. Pospelov and A. Ritz, *Higgs decays to dark matter: beyond the minimal model*, *Phys. Rev.* **D84** (2011) 113001, [[arXiv:1109.4872](#)].

78. I. Low, P. Schwaller, G. Shaughnessy, and C. E. M. Wagner, *The dark side of the Higgs boson*, *Phys. Rev.* **D85** (2012) 015009, [[arXiv:1110.4405](#)].

79. O. Lebedev, H. M. Lee, and Y. Mambrini, *Vector Higgs-portal dark matter and the invisible Higgs*, *Phys. Lett.* **B707** (2012) 570–576, [[arXiv:1111.4482](#)].

80. A. Djouadi, O. Lebedev, Y. Mambrini, and J. Quevillon, *Implications of LHC searches for Higgs-portal dark matter*, *Phys. Lett.* **B709** (2014) 65–69, [[arXiv:1112.3299](#)].

81. J. F. Kamenik and C. Smith, *Could a light Higgs boson illuminate the dark sector?*, *Phys. Rev.* **D85** (2012) 093017, [[arXiv:1201.4814](#)].

82. L. Lopez-Honorez, T. Schwetz, and J. Zupan, *Higgs portal, fermionic dark matter, and a Standard Model like Higgs at 125 GeV*, *Phys. Lett.* **B716** (2014) 179–185, [[arXiv:1203.2064](#)].

83. A. Djouadi, A. Falkowski, Y. Mambrini, and J. Quevillon, *Direct Detection of Higgs-Portal Dark Matter at the LHC*, *Eur. Phys. J.* **C73** (2013), no. 6 2455, [[arXiv:1205.3169](#)].

84. A. Greljo, J. Julio, J. F. Kamenik, C. Smith, and J. Zupan, *Constraining Higgs mediated dark matter interactions*, *JHEP* **11** (2013) 190, [[arXiv:1309.3561](#)].

85. A. A. Petrov and W. Shepherd, *Searching for dark matter at LHC with Mono-Higgs production*, *Phys. Lett.* **B730** (2014) 178–183, [[arXiv:1311.1511](#)].

86. L. Carpenter, A. DiFranzo, M. Mulhearn, C. Shimmin, S. Tulin, and D. Whiteson, *Mono-Higgs-boson: A new collider probe of dark matter*, *Phys. Rev.* **D89** (2014), no. 7 075017, [[arXiv:1312.2592](#)].

87. A. Alves, S. Profumo, and F. S. Queiroz, *The dark Z' portal: direct, indirect and collider searches*, *JHEP* **04** (2014) 063, [[arXiv:1312.5281](#)].

88. G. Arcadi, Y. Mambrini, M. H. G. Tytgat, and B. Zaldivar, *Invisible Z' and dark matter: LHC vs LUX constraints*, *JHEP* **03** (2014) 134, [[arXiv:1401.0221](#)].

89. A. Crivellin, F. D’Eramo, and M. Procura, *New Constraints on Dark Matter Effective Theories from Standard Model Loops*, *Phys. Rev. Lett.* **112** (2014) 191304, [[arXiv:1402.1173](#)].

90. N. F. Bell, Y. Cai, J. B. Dent, R. K. Leane, and T. J. Weiler, *Dark matter at the LHC: Effective field theories and gauge invariance*, *Phys. Rev.* **D92** (2015), no. 5 053008, [[arXiv:1503.07874](#)].

91. Y. Bai, J. Bourbeau, and T. Lin, *Dark matter searches with a mono- Z' jet*, *JHEP* **06** (2015) 205, [[arXiv:1504.01395](#)].

92. A. Crivellin, U. Haisch, and A. Hibbs, *LHC constraints on gauge boson couplings to dark matter*, *Phys. Rev.* **D91** (2015) 074028, [[arXiv:1501.00907](https://arxiv.org/abs/1501.00907)].

93. CMS Collaboration, V. Khachatryan et al., *Search for the production of dark matter in association with top-quark pairs in the single-lepton final state in proton-proton collisions at $\sqrt{s} = 8$ TeV*, *JHEP* **06** (2015) 121, [[arXiv:1504.03198](https://arxiv.org/abs/1504.03198)].

94. CMS Collaboration, V. Khachatryan et al., *Search for physics beyond the standard model in final states with a lepton and missing transverse energy in proton-proton collisions at $\sqrt{s} = 8$ TeV*, *Phys. Rev.* **D91** (2015), no. 9 092005, [[arXiv:1408.2745](https://arxiv.org/abs/1408.2745)].

95. CMS Collaboration, V. Khachatryan et al., *Search for new phenomena in monophoton final states in proton-proton collisions at $\sqrt{s} = 8$ TeV*, *Phys. Lett.* **B755** (2016) 102–124, [[arXiv:1410.8812](https://arxiv.org/abs/1410.8812)].

96. CMS Collaboration, V. Khachatryan et al., *Search for dark matter, extra dimensions, and unparticles in monojet events in proton?proton collisions at $\sqrt{s} = 8$ TeV*, *Eur. Phys. J.* **C75** (2015), no. 5 235, [[arXiv:1408.3583](https://arxiv.org/abs/1408.3583)].

97. ATLAS Collaboration, G. Aad et al., *Search for dark matter in events with heavy quarks and missing transverse momentum in pp collisions with the ATLAS detector*, *Eur. Phys. J.* **C75** (2015), no. 2 92, [[arXiv:1410.4031](https://arxiv.org/abs/1410.4031)].

98. ATLAS Collaboration, G. Aad et al., *Search for dark matter in events with a hadronically decaying W or Z boson and missing transverse momentum in pp collisions at $\sqrt{s} = 8$ TeV with the ATLAS detector*, *Phys. Rev. Lett.* **112** (2014), no. 4 041802, [[arXiv:1309.4017](https://arxiv.org/abs/1309.4017)].

99. ATLAS Collaboration, G. Aad et al., *Search for dark matter in events with a Z boson and missing transverse momentum in pp collisions at $\sqrt{s}=8$ TeV with the ATLAS detector*, *Phys. Rev.* **D90** (2014), no. 1 012004, [[arXiv:1404.0051](https://arxiv.org/abs/1404.0051)].

100. ATLAS Collaboration, G. Aad et al., *Search for new particles in events with one lepton and missing transverse momentum in pp collisions at $\sqrt{s} = 8$ TeV with the ATLAS detector*, *JHEP* **09** (2014) 037, [[arXiv:1407.7494](https://arxiv.org/abs/1407.7494)].

101. ATLAS Collaboration, G. Aad et al., *Search for new phenomena in events with a photon and missing transverse momentum in pp collisions at $\sqrt{s} = 8$ TeV with the ATLAS detector*, *Phys. Rev.* **D91** (2015), no. 1 012008, [[arXiv:1411.1559](https://arxiv.org/abs/1411.1559)]. [Erratum: *Phys. Rev.* D92,no.5,059903(2015)].

102. ATLAS Collaboration, G. Aad et al., *Search for new phenomena in final states with an energetic jet and large missing transverse momentum in pp collisions at $\sqrt{s} = 8$ TeV with the ATLAS detector*, *Eur. Phys. J.* **C75** (2015), no. 7 299, [[arXiv:1502.01518](https://arxiv.org/abs/1502.01518)]. [Erratum: *Eur. Phys. J.* C75,no.9,408(2015)].

103. S. Liem, G. Bertone, F. Calore, R. R. de Austri, T. M. P. Tait, R. Trotta, and C. Weniger, *Effective Field Theory of Dark Matter: a Global Analysis*, [[arXiv:1603.05994](https://arxiv.org/abs/1603.05994)].

104. N. Lopez, L. M. Carpenter, R. Cotta, M. Frate, N. Zhou, and D. Whiteson, *Collider Bounds on Indirect Dark Matter Searches: The WW Final State*, *Phys. Rev.* **D89** (2014), no. 11 115013, [[arXiv:1403.6734](https://arxiv.org/abs/1403.6734)].

105. G. Busoni, A. De Simone, T. Jacques, E. Morgante, and A. Riotto, *On the Validity of the Effective Field Theory for Dark Matter Searches at the LHC Part III: Analysis for the t-channel*, *JCAP* **1409** (2014) 022, [[arXiv:1405.3101](https://arxiv.org/abs/1405.3101)].

106. J. Abdallah et al., *Simplified Models for Dark Matter and Missing Energy Searches at the LHC*, [[arXiv:1409.2893](https://arxiv.org/abs/1409.2893)].

107. S. A. Malik et al., *Interplay and Characterization of Dark Matter Searches at Colliders and in Direct Detection Experiments*, *Phys. Dark Univ.* **9-10** (2015) 51–58,

[[arXiv:1409.4075](https://arxiv.org/abs/1409.4075)].

108. J. Abdallah et al., *Simplified Models for Dark Matter Searches at the LHC*, *Phys. Dark Univ.* **9-10** (2015) 8–23, [[arXiv:1506.03116](https://arxiv.org/abs/1506.03116)].

109. D. Abercrombie et al., *Dark Matter Benchmark Models for Early LHC Run-2 Searches: Report of the ATLAS/CMS Dark Matter Forum*, [arXiv:1507.00966](https://arxiv.org/abs/1507.00966).

110. A. Boveia et al., *Recommendations on presenting LHC searches for missing transverse energy signals using simplified s-channel models of dark matter*, [arXiv:1603.04156](https://arxiv.org/abs/1603.04156).

111. N. Arkani-Hamed, P. Schuster, N. Toro, J. Thaler, L.-T. Wang, B. Knuteson, and S. Mrenna, *MARMOSET: The Path from LHC Data to the New Standard Model via On-Shell Effective Theories*, [hep-ph/0703088](https://arxiv.org/abs/hep-ph/0703088).

112. J. Alwall, P. Schuster, and N. Toro, *Simplified Models for a First Characterization of New Physics at the LHC*, *Phys. Rev.* **D79** (2009) 075020, [[arXiv:0810.3921](https://arxiv.org/abs/0810.3921)].

113. **LHC New Physics Working Group** Collaboration, D. Alves, *Simplified Models for LHC New Physics Searches*, *J. Phys.* **G39** (2012) 105005, [[arXiv:1105.2838](https://arxiv.org/abs/1105.2838)].

114. A. De Simone, G. F. Giudice, and A. Strumia, *Benchmarks for Dark Matter Searches at the LHC*, *JHEP* **06** (2014) 081, [[arXiv:1402.6287](https://arxiv.org/abs/1402.6287)].

115. N. F. Bell, Y. Cai, and R. K. Leane, *Mono-W Dark Matter Signals at the LHC: Simplified Model Analysis*, *JCAP* **1601** (2016), no. 01 051, [[arXiv:1512.00476](https://arxiv.org/abs/1512.00476)].

116. U. Haisch, F. Kahlhoefer, and T. M. P. Tait, *On Mono-W Signatures in Spin-1 Simplified Models*, [arXiv:1603.01267](https://arxiv.org/abs/1603.01267).

117. M. Endo and Y. Yamamoto, *Unitarity Bounds on Dark Matter Effective Interactions at LHC*, *JHEP* **06** (2014) 126, [[arXiv:1403.6610](https://arxiv.org/abs/1403.6610)].

118. D. Racco, A. Wulzer, and F. Zwirner, *Robust collider limits on heavy-mediator Dark Matter*, *JHEP* **05** (2015) 009, [[arXiv:1502.04701](https://arxiv.org/abs/1502.04701)].

119. A. Berlin, T. Lin, and L.-T. Wang, *Mono-Higgs Detection of Dark Matter at the LHC*, *JHEP* **06** (2014) 078, [[arXiv:1402.7074](https://arxiv.org/abs/1402.7074)].

120. *Sensitivity to WIMP Dark Matter in the Final States Containing Jets and Missing Transverse Momentum with the ATLAS Detector at 14 TeV LHC*, Tech. Rep. ATL-PHYS-PUB-2014-007, CERN, Geneva, Jun, 2014.

121. M. Cirelli, E. Del Nobile, and P. Panci, *Tools for model-independent bounds in direct dark matter searches*, *JCAP* **1310** (2013) 019, [[arXiv:1307.5955](https://arxiv.org/abs/1307.5955)].

122. F. D’Eramo and M. Procura, *Connecting Dark Matter UV Complete Models to Direct Detection Rates via Effective Field Theory*, *JHEP* **04** (2015) 054, [[arXiv:1411.3342](https://arxiv.org/abs/1411.3342)].

123. G. Belanger, F. Boudjema, A. Pukhov, and A. Semenov, *micrOMEGAs_3.1: A program for calculating dark matter observables*, *Comput. Phys. Commun.* **185** (2014) 960–985, [[arXiv:1305.0237](https://arxiv.org/abs/1305.0237)].

124. J. R. Ellis, A. Ferstl, and K. A. Olive, *Reevaluation of the elastic scattering of supersymmetric dark matter*, *Phys. Lett.* **B481** (2000) 304–314, [[hep-ph/0001005](https://arxiv.org/abs/hep-ph/0001005)].

125. P. Gondolo, J. Edsjo, P. Ullio, L. Bergstrom, M. Schelke, and E. A. Baltz, *DarkSUSY: Computing supersymmetric dark matter properties numerically*, *JCAP* **0407** (2004) 008, [[astro-ph/0406204](https://arxiv.org/abs/astro-ph/0406204)].

126. J. R. Ellis, K. A. Olive, and C. Savage, *Hadronic Uncertainties in the Elastic Scattering of Supersymmetric Dark Matter*, *Phys. Rev.* **D77** (2008) 065026, [[arXiv:0801.3656](https://arxiv.org/abs/0801.3656)].

127. G. Belanger, F. Boudjema, A. Pukhov, and A. Semenov, *Dark matter direct detection rate in a generic model with micrOMEGAs 2.2*, *Comput. Phys. Commun.* **180** (2009) 747–767, [[arXiv:0803.2360](https://arxiv.org/abs/0803.2360)].

128. H.-Y. Cheng and C.-W. Chiang, *Revisiting Scalar and Pseudoscalar Couplings with Nucleons*, *JHEP* **07** (2012) 009, [[arXiv:1202.1292](#)].

129. M. Anselmino, M. Boglione, U. D'Alesio, A. Kotzinian, F. Murgia, A. Prokudin, and S. Melis, *Update on transversity and Collins functions from SIDIS and $e^+ e^-$ data*, *Nucl. Phys. Proc. Suppl.* **191** (2009) 98–107, [[arXiv:0812.4366](#)].

130. M. Anselmino, M. Boglione, U. D'Alesio, S. Melis, F. Murgia, and A. Prokudin, *Simultaneous extraction of transversity and Collins functions from new SIDIS and $e^+ e^-$ data*, *Phys. Rev.* **D87** (2013) 094019, [[arXiv:1303.3822](#)].

131. A. Bacchetta, A. Courtoy, and M. Radici, *First extraction of valence transversities in a collinear framework*, *JHEP* **03** (2013) 119, [[arXiv:1212.3568](#)].

132. M. Cirelli, *Status of Indirect (and Direct) Dark Matter searches*, [arXiv:1511.02031](#).

133. M. Cirelli, G. Corcella, A. Hektor, G. Hutsi, M. Kadastik, P. Panci, M. Raidal, F. Sala, and A. Strumia, *PPPC 4 DM ID: A Poor Particle Physicist Cookbook for Dark Matter Indirect Detection*, *JCAP* **1103** (2011) 051, [[arXiv:1012.4515](#)]. [Erratum: *JCAP*1210,E01(2012)].

134. A. Alves, S. Profumo, F. S. Queiroz, and W. Shepherd, *Effective field theory approach to the Galactic Center gamma-ray excess*, *Phys. Rev.* **D90** (2014), no. 11 115003, [[arXiv:1403.5027](#)].

135. A. Rajaraman, T. M. P. Tait, and A. M. Wijangco, *Effective Theories of Gamma-ray Lines from Dark Matter Annihilation*, *Phys. Dark Univ.* **2** (2013) 17–21, [[arXiv:1211.7061](#)].

136. M. Gustafsson, T. Hambye, and T. Scarna, *Effective Theory of Dark Matter Decay into Monochromatic Photons and its Implications: Constraints from Associated Cosmic-Ray Emission*, *Phys. Lett.* **B724** (2013) 288–295, [[arXiv:1303.4423](#)].

137. G. Ovanesyan, T. R. Slatyer, and I. W. Stewart, *Heavy Dark Matter Annihilation from Effective Field Theory*, *Phys. Rev. Lett.* **114** (2015), no. 21 211302, [[arXiv:1409.8294](#)].

138. A. Rajaraman, T. M. P. Tait, and D. Whiteson, *Two Lines or Not Two Lines? That is the Question of Gamma Ray Spectra*, *JCAP* **1209** (2012) 003, [[arXiv:1205.4723](#)].

139. Y.-L. S. Tsai, Q. Yuan, and X. Huang, *A generic method to constrain the dark matter model parameters from Fermi observations of dwarf spheroids*, *JCAP* **1303** (2013) 018, [[arXiv:1212.3990](#)].

140. L. M. Carpenter, R. Colburn, and J. Goodman, *Indirect Detection Constraints on the Model Space of Dark Matter Effective Theories*, *Phys. Rev.* **D92** (2015), no. 9 095011, [[arXiv:1506.08841](#)].

141. D. Chowdhury, A. M. Iyer, and R. Laha, *Constraints on dark matter annihilation to fermions and a photon*, [arXiv:1601.06140](#).

142. L. Bergstrom, *Radiative Processes in Dark Matter Photino Annihilation*, *Phys. Lett.* **B225** (1989) 372.

143. T. Bringmann, L. Bergstrom, and J. Edsjo, *New Gamma-Ray Contributions to Supersymmetric Dark Matter Annihilation*, *JHEP* **01** (2008) 049, [[arXiv:0710.3169](#)].

144. L. Bergstrom, T. Bringmann, and J. Edsjo, *New Positron Spectral Features from Supersymmetric Dark Matter - a Way to Explain the PAMELA Data?*, *Phys. Rev.* **D78** (2008) 103520, [[arXiv:0808.3725](#)].

145. P. Ciafaloni, D. Comelli, A. Riotto, F. Sala, A. Strumia, and A. Urbano, *Weak Corrections are Relevant for Dark Matter Indirect Detection*, *JCAP* **1103** (2011) 019, [[arXiv:1009.0224](#)].

146. N. F. Bell, J. B. Dent, T. D. Jacques, and T. J. Weiler, *W/Z Bremsstrahlung as the Dominant Annihilation Channel for Dark Matter*, *Phys. Rev.* **D83** (2011) 013001, [[arXiv:1009.2584](https://arxiv.org/abs/1009.2584)].

147. N. F. Bell, J. B. Dent, T. D. Jacques, and T. J. Weiler, *Dark Matter Annihilation Signatures from Electroweak Bremsstrahlung*, *Phys. Rev.* **D84** (2011) 103517, [[arXiv:1101.3357](https://arxiv.org/abs/1101.3357)].

148. P. Ciafaloni, M. Cirelli, D. Comelli, A. De Simone, A. Riotto, and A. Urbano, *On the Importance of Electroweak Corrections for Majorana Dark Matter Indirect Detection*, *JCAP* **1106** (2011) 018, [[arXiv:1104.2996](https://arxiv.org/abs/1104.2996)].

149. N. F. Bell, J. B. Dent, A. J. Galea, T. D. Jacques, L. M. Krauss, and T. J. Weiler, *W/Z Bremsstrahlung as the Dominant Annihilation Channel for Dark Matter, Revisited*, *Phys. Lett.* **B706** (2011) 6–12, [[arXiv:1104.3823](https://arxiv.org/abs/1104.3823)].

150. M. Garny, A. Ibarra, and S. Vogl, *Antiproton constraints on dark matter annihilations from internal electroweak bremsstrahlung*, *JCAP* **1107** (2011) 028, [[arXiv:1105.5367](https://arxiv.org/abs/1105.5367)].

151. P. Ciafaloni, M. Cirelli, D. Comelli, A. De Simone, A. Riotto, and A. Urbano, *Initial State Radiation in Majorana Dark Matter Annihilations*, *JCAP* **1110** (2011) 034, [[arXiv:1107.4453](https://arxiv.org/abs/1107.4453)].

152. A. Hryczuk and R. Iengo, *The one-loop and Sommerfeld electroweak corrections to the Wino dark matter annihilation*, *JHEP* **01** (2012) 163, [[arXiv:1111.2916](https://arxiv.org/abs/1111.2916)]. [Erratum: *JHEP* **06**, 137 (2012)].

153. V. Barger, W.-Y. Keung, and D. Marfatia, *Bremsstrahlung in dark matter annihilation*, *Phys. Lett.* **B707** (2012) 385–388, [[arXiv:1111.4523](https://arxiv.org/abs/1111.4523)].

154. M. Garny, A. Ibarra, and S. Vogl, *Dark matter annihilations into two light fermions and one gauge boson: General analysis and antiproton constraints*, *JCAP* **1204** (2012) 033, [[arXiv:1112.5155](https://arxiv.org/abs/1112.5155)].

155. A. De Simone, *Electroweak lights from Dark Matter annihilations*, *J. Phys. Conf. Ser.* **375** (2012) 012046, [[arXiv:1201.1443](https://arxiv.org/abs/1201.1443)].

156. IceCube Collaboration, M. G. Aartsen et al., *Improved limits on dark matter annihilation in the Sun with the 79-string IceCube detector and implications for supersymmetry*, [arXiv:1601.00653](https://arxiv.org/abs/1601.00653).

157. G. D’Ambrosio, G. F. Giudice, G. Isidori, and A. Strumia, *Minimal flavor violation: An Effective field theory approach*, *Nucl. Phys.* **B645** (2002) 155–187, [[hep-ph/0207036](https://arxiv.org/abs/hep-ph/0207036)].

158. T. Hambye and A. Strumia, *Dynamical generation of the weak and Dark Matter scale*, *Phys. Rev.* **D88** (2013) 055022, [[arXiv:1306.2329](https://arxiv.org/abs/1306.2329)].

159. V. V. Khoze, C. McCabe, and G. Ro, *Higgs vacuum stability from the dark matter portal*, *JHEP* **08** (2014) 026, [[arXiv:1403.4953](https://arxiv.org/abs/1403.4953)].

160. W. Altmannshofer, W. A. Bardeen, M. Bauer, M. Carena, and J. D. Lykken, *Light Dark Matter, Naturalness, and the Radiative Origin of the Electroweak Scale*, *JHEP* **01** (2015) 032, [[arXiv:1408.3429](https://arxiv.org/abs/1408.3429)].

161. S. R. Coleman and E. J. Weinberg, *Radiative Corrections as the Origin of Spontaneous Symmetry Breaking*, *Phys. Rev.* **D7** (1973) 1888–1910.

162. K. A. Meissner and H. Nicolai, *Conformal Symmetry and the Standard Model*, *Phys. Lett.* **B648** (2007) 312–317, [[hep-th/0612165](https://arxiv.org/abs/hep-th/0612165)].

163. R. Foot, A. Kobakhidze, K. L. McDonald, and R. R. Volkas, *A Solution to the hierarchy problem from an almost decoupled hidden sector within a classically scale invariant theory*, *Phys. Rev.* **D77** (2008) 035006, [[arXiv:0709.2750](https://arxiv.org/abs/0709.2750)].

164. C. Englert, J. Jaeckel, V. V. Khoze, and M. Spannowsky, *Emergence of the Electroweak Scale through the Higgs Portal*, *JHEP* **04** (2013) 060, [[arXiv:1301.4224](https://arxiv.org/abs/1301.4224)].

165. V. Barger, P. Langacker, M. McCaskey, M. J. Ramsey-Musolf, and G. Shaughnessy, *LHC Phenomenology of an Extended Standard Model with a Real Scalar Singlet*, *Phys. Rev.* **D77** (2008) 035005, [[arXiv:0706.4311](https://arxiv.org/abs/0706.4311)].

166. J. M. Cline, K. Kainulainen, P. Scott, and C. Weniger, *Update on scalar singlet dark matter*, *Phys. Rev.* **D88** (2013) 055025, [[arXiv:1306.4710](https://arxiv.org/abs/1306.4710)]. [Erratum: *Phys. Rev.* **D92**, no. 3, 039906 (2015)].

167. N. Craig, H. K. Lou, M. McCullough, and A. Thalapillil, *The Higgs Portal Above Threshold*, [arXiv:1412.0258](https://arxiv.org/abs/1412.0258).

168. J. Ellis, *TikZ-Feynman: Feynman diagrams with TikZ*, [arXiv:1601.05437](https://arxiv.org/abs/1601.05437).

169. Y. G. Kim, K. Y. Lee, and S. Shin, *Singlet fermionic dark matter*, *JHEP* **05** (2008) 100, [[arXiv:0803.2932](https://arxiv.org/abs/0803.2932)].

170. S. Baek, P. Ko, and W.-I. Park, *Search for the Higgs portal to a singlet fermionic dark matter at the LHC*, *JHEP* **02** (2012) 047, [[arXiv:1112.1847](https://arxiv.org/abs/1112.1847)].

171. LUX Collaboration, D. S. Akerib et al., *Improved WIMP scattering limits from the LUX experiment*, [arXiv:1512.03506](https://arxiv.org/abs/1512.03506).

172. G. Belanger, B. Dumont, U. Ellwanger, J. F. Gunion, and S. Kraml, *Status of invisible Higgs decays*, *Phys. Lett.* **B723** (2013) 340–347, [[arXiv:1302.5694](https://arxiv.org/abs/1302.5694)].

173. A. Farzinnia, H.-J. He, and J. Ren, *Natural Electroweak Symmetry Breaking from Scale Invariant Higgs Mechanism*, *Phys. Lett.* **B727** (2013) 141–150, [[arXiv:1308.0295](https://arxiv.org/abs/1308.0295)].

174. B. A. Dobrescu, K. Kong, and R. Mahbubani, *Leptons and photons at the LHC: Cascades through spinless adjoints*, *JHEP* **07** (2007) 006, [[hep-ph/0703231](https://arxiv.org/abs/hep-ph/0703231)].

175. B. A. Dobrescu, K. Kong, and R. Mahbubani, *Massive color-octet bosons and pairs of resonances at hadron colliders*, *Phys. Lett.* **B670** (2008) 119–123, [[arXiv:0709.2378](https://arxiv.org/abs/0709.2378)].

176. ATLAS Collaboration, G. Aad et al., *ATLAS search for new phenomena in dijet mass and angular distributions using pp collisions at $\sqrt{s} = 7$ TeV*, *JHEP* **01** (2013) 029, [[arXiv:1210.1718](https://arxiv.org/abs/1210.1718)].

177. J. Kile, *Flavored Dark Matter: A Review*, *Mod. Phys. Lett.* **A28** (2013) 1330031, [[arXiv:1308.0584](https://arxiv.org/abs/1308.0584)].

178. P. Agrawal, B. Batell, D. Hooper, and T. Lin, *Flavored Dark Matter and the Galactic Center Gamma-Ray Excess*, *Phys. Rev.* **D90** (2014), no. 6 063512, [[arXiv:1404.1373](https://arxiv.org/abs/1404.1373)].

179. M. Garny, A. Ibarra, and S. Vogl, *Signatures of Majorana dark matter with t -channel mediators*, *Int. J. Mod. Phys.* **D24** (2015), no. 07 1530019, [[arXiv:1503.01500](https://arxiv.org/abs/1503.01500)].

180. M. Garny, A. Ibarra, S. Rydbeck, and S. Vogl, *Majorana Dark Matter with a Coloured Mediator: Collider vs Direct and Indirect Searches*, *JHEP* **06** (2014) 169, [[arXiv:1403.4634](https://arxiv.org/abs/1403.4634)].

181. M. Papucci, A. Vichi, and K. M. Zurek, *Monojet versus the rest of the world I: t -channel models*, *JHEP* **11** (2014) 024, [[arXiv:1402.2285](https://arxiv.org/abs/1402.2285)].

182. AMS Collaboration, L. Accardo et al., *High Statistics Measurement of the Positron Fraction in Primary Cosmic Rays of 0.5?500 GeV with the Alpha Magnetic Spectrometer on the International Space Station*, *Phys. Rev. Lett.* **113** (2014) 121101.

183. Fermi-LAT Collaboration, M. Ackermann et al., *Measurement of separate cosmic-ray electron and positron spectra with the Fermi Large Area Telescope*, *Phys. Rev. Lett.* **108** (2012) 011103, [[arXiv:1109.0521](https://arxiv.org/abs/1109.0521)].

184. **AMS** Collaboration, M. Aguilar et al., *Precision Measurement of the Proton Flux in Primary Cosmic Rays from Rigidity 1 GV to 1.8 TV with the Alpha Magnetic Spectrometer on the International Space Station*, *Phys. Rev. Lett.* **114** (2015) 171103.

185. F. Giacchino, A. Ibarra, L. L. Honorez, M. H. G. Tytgat, and S. Wild, *Signatures from Scalar Dark Matter with a Vector-like Quark Mediator*, *JCAP* **1602** (2016), no. 02 002, [[arXiv:1511.04452](https://arxiv.org/abs/1511.04452)].

186. T. Toma, *Internal Bremsstrahlung Signature of Real Scalar Dark Matter and Consistency with Thermal Relic Density*, *Phys. Rev. Lett.* **111** (2013) 091301, [[arXiv:1307.6181](https://arxiv.org/abs/1307.6181)].

187. F. Giacchino, L. Lopez-Honorez, and M. H. G. Tytgat, *Scalar Dark Matter Models with Significant Internal Bremsstrahlung*, *JCAP* **1310** (2013) 025, [[arXiv:1307.6480](https://arxiv.org/abs/1307.6480)].

188. **CMS** Collaboration, S. Chatrchyan et al., *Inclusive search for a vector-like T quark with charge $\frac{2}{3}$ in pp collisions at $\sqrt{s} = 8$ TeV*, *Phys. Lett. B* **729** (2014) 149–171, [[arXiv:1311.7667](https://arxiv.org/abs/1311.7667)].

189. **ATLAS** Collaboration, G. Aad et al., *Search for production of vector-like quark pairs and of four top quarks in the lepton-plus-jets final state in pp collisions at $\sqrt{s} = 8$ TeV with the ATLAS detector*, *JHEP* **08** (2015) 105, [[arXiv:1505.04306](https://arxiv.org/abs/1505.04306)].

190. J. Hisano, R. Nagai, and N. Nagata, *Effective Theories for Dark Matter Nucleon Scattering*, *JHEP* **05** (2015) 037, [[arXiv:1502.02244](https://arxiv.org/abs/1502.02244)].

191. **ATLAS** Collaboration, G. Aad et al., *Summary of the searches for squarks and gluinos using $\sqrt{s} = 8$ TeV pp collisions with the ATLAS experiment at the LHC*, *JHEP* **10** (2015) 054, [[arXiv:1507.05525](https://arxiv.org/abs/1507.05525)].

192. F. Kahlhoefer, K. Schmidt-Hoberg, T. Schwetz, and S. Vogl, *Implications of unitarity and gauge invariance for simplified dark matter models*, [arXiv:1510.02110](https://arxiv.org/abs/1510.02110).

193. M. Chala, F. Kahlhoefer, M. McCullough, G. Nardini, and K. Schmidt-Hoberg, *Constraining Dark Sectors with Monojets and Dijets*, *JHEP* **07** (2015) 089, [[arXiv:1503.05916](https://arxiv.org/abs/1503.05916)].

194. T. Jacques and K. Nordström, *Mapping monojet constraints onto Simplified Dark Matter Models*, *JHEP* **06** (2015) 142, [[arXiv:1502.05721](https://arxiv.org/abs/1502.05721)].

195. A. J. Brennan, M. F. McDonald, J. Gramling, and T. D. Jacques, *Collide and Conquer: Constraints on Simplified Dark Matter Models using Mono-X Collider Searches*, [arXiv:1603.01366](https://arxiv.org/abs/1603.01366).

196. O. Lebedev and Y. Mambrini, *Axial dark matter: The case for an invisible Z?*, *Phys. Lett. B* **734** (2014) 350–353, [[arXiv:1403.4837](https://arxiv.org/abs/1403.4837)].

197. R. Mahbubani and L. Senatore, *The Minimal model for dark matter and unification*, *Phys. Rev. D* **73** (2006) 043510, [[hep-ph/0510064](https://arxiv.org/abs/hep-ph/0510064)].

198. R. Enberg, P. J. Fox, L. J. Hall, A. Y. Papaioannou, and M. Papucci, *LHC and dark matter signals of improved naturalness*, *JHEP* **11** (2007) 014, [[arXiv:0706.0918](https://arxiv.org/abs/0706.0918)].

199. T. Cohen, J. Kearney, A. Pierce, and D. Tucker-Smith, *Singlet-Doublet Dark Matter*, *Phys. Rev. D* **85** (2012) 075003, [[arXiv:1109.2604](https://arxiv.org/abs/1109.2604)].

200. L. Calibbi, A. Mariotti, and P. Tziveloglou, *Singlet-Doublet Model: Dark matter searches and LHC constraints*, *JHEP* **10** (2015) 116, [[arXiv:1505.03867](https://arxiv.org/abs/1505.03867)].